ARL-CR-141
NASA CR 194450
UTRC REPORT R93-958160-1

STUDY OF STREAMWISE VORTICITY-STIRRED COMBUSTION

William T. Peschke and John B. McVey
United Technologies Research Center
East Hartford, Connecticut

December 1993

Prepared for
U. S. Army Research Office
Under Contract DAAL03-89-C-0018

DISCLAIMER NOTICE

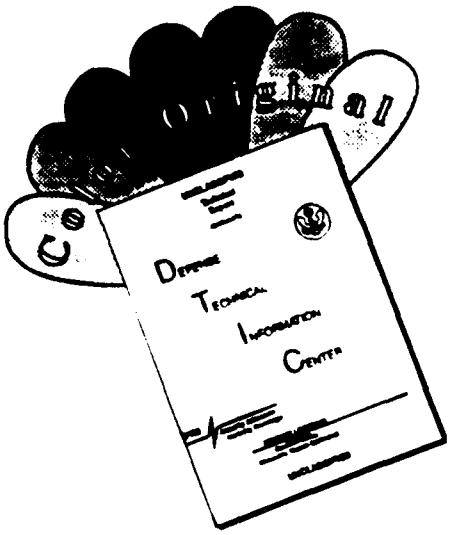

THIS DOCUMENT IS BEST QUALITY AVAILABLE. THE COPY FURNISHED TO DTIC CONTAINED A SIGNIFICANT NUMBER OF COLOR PAGES WHICH DO NOT REPRODUCE LEGIBLY ON BLACK AND WHITE MICROFICHE.

Study of Streamwise Vorticity-Stirred Combustion

Table of Contents

STUDY OF STREAMWISE VORTICITY-STIRRED COMBUSTION

Final Report

ABSTRACT

Experiments were conducted to establish the effects of the introduction of streamwise vorticity in combusting flows modelling those developed within small gas turbine engines. The objective of the effort was to determine whether this combustion concept has the potential for improving the volumetric heat release rates that characterize these engines. Water flow-visualization tests were performed to evolve lobed mixer configurations that, while generating vortex arrays within both the primary and secondary streams, would also provide rapid intermixing between the streams. These experiments resulted in the definition of enhanced-mixing configurations that were characterized, according to air bubble and dye trajectories, by strong interactions between the two streams. These interactions induced a substantial vertical interchange of primary and secondary fluids. Intermingling of the two fluids occurred throughout a region covering 80 percent of the height of the duct within distances from the lobe mixer trailing edge ranging from approximately one-half to one duct height.

Combustion experiments were carried out in a high-pressure (7 atm) combustion apparatus using lobe-mixer combinations that exhibited the ability to induce rapid interchange between the primary and secondary streams. Direct observation and gas sampling were employed to characterize the fuel-air ratio distribution effected by the mixers. Flame geometries were compared with those developed during shear-layer combustion occurring downstream from a conventional splitter plate. The results show that the lobed mixers induce a rapid relocation of the fuel-air mixture entering the combustion test section. As contrasted with the 5- to 7-degree flame front angles that occurred during shear layer combustion, the flame front angles developed during combustion using the lobed mixers were more than twice as great, attaining levels approaching 20 degrees.

NOMENCLATURE

EI	Emissions index
E.R.	Fuel-air equivalence ratio
f/a	Fuel-air mass flow ratio
H	Overall height of duct
H_{lp}	Lobe height of primary lobe mixer
H_{ls}	Lobe height of secondary lobe mixer
H_{max}	Maximum height of mixed region denoted by dye traces
H_{st}	Height of rearward-facing step in primary flow
h_{st}	Height of rearward-facing step in secondary flow

L_{pri} Distance from step at which H_{max} is measured in primary flow

L_{sec} Distance from step at which H_{max} is measured in secondary flow

$L_{1/2}$ Distance from step in which one-half turn of the vortex occurs

M_i Molecular weight of species, i

$(Q_L)_i$ Lower heating value of species, i

Re Reynolds number

U_{pri} Primary flow velocity

U_{sec} Secondary flow velocity

W Overall width of duct

W_{pri} Primary weight flow rate

W_{sec} Secondary weight flow rate

X_i Mole fraction of species, i

INTRODUCTION

Recent investigations (Refs. 1,2) have shown that flame spreading rates attained using convoluted surfaces in combustion experiments are approximately twice the rates that characterize conventional shear-layer mixing associated with linear flow-splitter plates. The increased rates of flame spreading have been attributed to the effect of large-scale streaming vortices, induced in the flow by the convoluted splitters, on the fuel-air mixing process. The physical processes responsible for the generation of streamwise vorticity by a convoluted surface have been described previously, for example, in Refs. 1 through 5. A more recent investigation by McCormick (Ref. 6) has revealed the role in enhancing mixing played by the normal vortex that is shed periodically from the convoluted trailing edge of the splitter. McCormick also showed that the symmetric lobed mixer provides improved flow mixing relative to an asymmetric lobed mixer.

Referring to Fig. 1, as the flow proceeds over the convoluted surface, the pressure field developed by the splitter contour and the geometry of the confining enclosure (duct) cause a deflection of the flow to occur. The direction of this flow is from the crest of the splitter to the adjacent troughs. The important process is the inviscid effect of the pressure field. Although the flow in the boundary layer undergoes a greater degree of turning than the flow in the mainstream, there is no firm evidence that the boundary layer characteristics are important relative to the intensity and scale of the vortices generated.

The principal viscous effect is the departure of the flow from the surface at the trailing edge (the Kutta condition). This flow separation results in the development of regions of very high shear as the upward-deflected flow from beneath the surface contacts the downward-deflected flow from the upward surface. The corresponding vorticity which is developed is zero at the crest and trough of the lobe; maximum at the midspan, and the sense of rotation alternates from one side of each lobe to the other.

Immediately downstream from the splitter trailing edge, vortex rollup occurs wherein the above-described vortex line develops into discrete, large-scale vortices; each vortex is centered more or less at the location of maximum trailing edge vorticity. The formation of these discrete vortical flow structures is an inviscid occurrence and

should be predictable through analysis of the inviscid, rotational flow.

According to McCormick (Ref. 6), the normal vortex sheds periodically from the convoluted trailing edge of the lobed mixer and, in combination with the streamwise vorticity, plays a significant role in the enhanced-mixing process. This effect occurs as the normal vortex is deformed by the streamwise vortex into a "pinched-off" structure that is unstable and generates intense turbulence.

In the current program, symmetric lobed mixers were used in a flow visualization task and, subsequently, in a combustion experiment to assess the level of rapid interaction attainable between two streams representing the primary and secondary flows in a small gas turbine.

FLOW VISUALIZATION TESTING

A flow visualization test apparatus, using water as the flowing medium, was constructed and operated to examine the flow patterns produced by selected flow reactor configurations. In these configurations, a recirculating flow, to act as a flame-stabilization site, was established proximate to an intended primary combustion zone. A secondary flow was brought into contact with this primary flow to provide tempering of the primary zone combustion products. The overall objective was to achieve intense mixing within the primary zone as well as between the primary and secondary streams. The experiments resulted in the identification of enhanced-mixing configurations that were characterized, according to air-bubble and dye traces, by strong interactions between the primary and secondary flows.

EXPERIMENTAL APPARATUS

A photograph of the flow visualization test section is shown in Fig. 2 and a schematic diagram of the apparatus is shown in Fig. 3. All water flows are from left to right in these figures. The overall length of the acrylic test section is 191 cm. and the cross-section of the duct is 152 x 152 mm. Separate inlet ducts for secondary and primary flows are provided as shown, with the two flows separated by a horizontal splitter plate that extends from the flow-path entrances to the start of the mixing section. The flow through the lower channel of the duct, adjacent to the rearward-facing step, is referred to as the primary flow in this report; the upper channel flow is the secondary flow corresponding to the dilution-air flow in a gas turbine combustor. The length of the mixing section, which provides an unobstructed view of the mixing region through all sides of the test section, is 51 cm. A 11.4-cm. diameter quartz window at the end of the test section, at the right end of Fig. 3 provides the ability to look upstream into the mixing region. The circular window is placed downstream from a weir that turns the flow upward and maintains a positive backpressure in the test section during flow. A closeup photograph of a single four-lobe mixer installed in the primary flowpath is shown in Fig. 4. The secondary flowpath is provided by the area above the primary/secondary splitter, placed directly above the lobe mixer in this view. Allocation of the primary flow between the upper and lower zones of the primary flowpath was accomplished by flexing a primary-flow splitter to which the primary mixer was attached, as shown in Fig. 5. The flow through the primary and secondary channels is monitored using paddle-wheel flowmeters. The flow splitters and lobe mixers can be relocated vertically in 0.64 cm. increments. Axial locations of

mixers and splitter plates may also be varied from test-to-test.

TEST CONFIGURATIONS

Fourteen configurations involving various primary and secondary lobe-mixer combinations were examined during this phase of the program. The geometric features of the two lobe mixers that were used to constitute the various combinations are depicted in Fig. 6. Both lobe mixers were configured to provide a penetration (lobe amplitude as a percentage of the height of the duct or upstream flow area which is to be affected by the mixer) of 70 percent. The installed dimensions associated with each of these arrangements are tabulated in Table I, using the nomenclature delineated in Fig. 7.

The lobed mixers were fabricated using 1.3-mm. thick stainless steel sheet. Each mixer was composed of a number of elements that were welded together. The mixers used in the flow visualization tests were also employed in the combustion tests. The sheet thickness was selected to provide a balance between stiffness and workability. No special design consideration was applied relative to prevention of warpage due to thermal stresses which develop during combustion testing.

DATA ACQUISITION

The visual data that were acquired consisted of videotape recordings of the flowfield, illuminated using a HeNe laser to excite fluorescence of a yellow and/or pink fluorescein dye. The dye was introduced through a capillary tube at selected locations in the flow. A laser sheet, configured using cylindrical lenses in various arrangements, was used to illuminate selected areas of the flowfield. To provide visualization of the bubble tracks while viewing from the exit of the test section, a 12- to 25-mm wide laser sheet, passed through the test section in a direction normal to the flow direction was used. This sheet could be relocated axially to any distance downstream from the trailing edge of the mixer. To illuminate the dye trajectory, a thin (less than approximately 5 mm) sheet of illumination was used. The plane of this sheet was aligned in the flow direction, passing either vertically or horizontally through the flow. This sheet, when vertical could be traversed horizontally or, when horizontal, could be moved in the vertical direction. The visual data were recorded on videotape; in special cases, 35 mm photographic records were made.

The water flow rates were measured directly using paddle-wheel type flowmeters. Flowmeter frequencies were read on an event timer and recorded manually for data reduction at a later time.

TEST RESULTS

A summary of the flow conditions examined during this effort is provided in Table II. Included in the table are the characteristics of the vortical part of the flowfield upon which the assessments of the effectiveness of a configuration were made.

Single Lobe Mixers

Initial tests were performed with the single lobe mixer shown in Fig. 4, installed close to a 25-mm high rearward-facing step at the entrance to the test section. The objective of these initial experiments was two-fold, i.e., to determine whether a vortical flow could be established with a single mixer and to assess the effect of this flow on the recirculation region formed by

the flow passing over the rearward-facing step.

A single, 5.33-cm. high lobe mixer, installed so that its trailing edge was aligned with the 2.5-cm. high step was used for the initial studies. This arrangement was designated Baseline 1 (B1) in Table I. Subsequently, the mixer trailing edge was relocated 5 cm. downstream (Baseline 1, Alternate 1 or B1A1) and upstream (B1A2) from the rearward-facing step to examine the interaction of the vortical flow with the recirculating flow behind the step. As evidenced by the traces of the air bubbles in the flow, the single lobe induced the anticipated vorticity in the flow even under flow conditions during which the calculated velocities above and below the primary splitter, approaching the mixer, were essentially equal. When the lobe trailing edge was either aligned with or downstream from the step, the recirculation region was generally unaffected, with its length corresponding approximately to 7.5 to 8 step heights. Relocating the lobe trailing edge to a distance of 5 cm. upstream from the step resulted in a reduction of the recirculation zone length to approximately 6.9 step heights, signifying that for this geometry, an interaction between the vortex flowfield and the recirculation region had occurred.

The experimental results, based on the extent to which dye, introduced into either the primary or secondary flow, migrated into the adjacent flow, indicated that no substantial mixing between the two flows occurred. Dye injected into either of the two flows was unable to traverse the slip region between the two flows.

Dual Lobe Mixers

Experiments involving the use of two lobe mixers were conducted to evaluate the degree of mixing that could be attained if the streamwise vortex ensemble generated by one lobe mixer were permitted to interact with a second ensemble. It was presupposed that such an interaction could lead to a complete melding of the primary and secondary (dilution air) flowfields in a gas turbine combustor, leading to more satisfactory temperature distributions than can be derived from conventional (dilution jet) approaches. One of the arrangements that developed strong primary/secondary flow interactions is shown in the photograph of Fig. 8. In all, eleven arrangements of the two four-lobe mixers were examined for their ability to provide enhanced penetration of one flow into the other. Referring to Table I, these comprise Configurations B2 (Baseline 2) through B5 (Baseline 5). The first seven of these arrangements incorporated the smaller (3.56-cm. tall) lobe mixer in the primary flow and the larger (6.1-cm. tall) mixer in the secondary flow. In the last four experimental configurations, Baseline 3 through Baseline 5, the locations of the larger and smaller lobe mixers were interchanged.

One of the mixer configurations, B3 (Baseline 3) incorporating both of the convoluted splitters, comprised an arrangement in which the lobes of the two mixers were out of phase with respect to one another. That is, the peaks of the lower splitter were installed adjacent to the valleys of the upper splitter, thereby directing the primary and secondary flows toward one another. This arrangement induced no apparent mixing of the two streams to occur.

Several of the lobe mixer arrangements induced rapid intermingling of the primary and secondary streams. Based on the dye and air bubble track visualization, it was determined that strong

interactions involving exchange of fluid between the primary and secondary flows could be made to occur when the distance separating the primary and secondary lobes was not greater than approximately 10 mm. A criterion was established for the ranking of configurations in terms of the extent of spreading of the dyed fluid relative to the height of the lobe mixer. Referring to Fig. 9, the quotients, H_{max}/H_L were calculated in Table I and those configurations exhibiting the greatest values of this parameter were subsequently selected for the combustion investigations. The quantity, H_{max} is the maximum vertical width attained by the dye envelope, measured from the videotape records. The parameter, H_L is the peak-to-peak height of the lobe mixer. In general, these configurations also exhibited the greatest values of the quotient, $H_{max}/L_{1/2}$. where the quantity, $L_{1/2}$ is the distance, measured from the trailing edge of the lobe, to the point where one-half of a revolution of the vortex has occurred. These values are also calculated and tabulated in Table II.

The air bubble tracks also revealed the presence of between three and four separate vortex structures within the recirculation zone induced by the flow over the rearward-facing step. The length of the recirculation zone varied from 5 to 7 step heights, a result consistent with other data found in the open literature.

Observations of the air-bubble trajectories provided evidence of the occurrence of the strong interactions between the primary and secondary flowfields and the existence and location of the induced vortices. Photographs of some of these bubble trajectories are presented as Figs. 10 and 11. A 2.5-cm. wide laser sheet was positioned normal to the flow at various distances downstream from the lobe mixer trailing edge to provide indications of the transverse flow components developed in this region. In Fig. 10, the laser sheet was positioned at a distance of 2.5 cm. from the lobe trailing edge and at a distance of 7.5 cm. from the trailing edge in Fig. 11. The right side of the cross-section, including the far right lobe, is not illuminated as brightly as the rest of the flowfield, owing to the optical setup used. Nevertheless, the videotape record shows a strong interaction occurring between the primary and secondary flows. The interaction comprises mass exchange between the primary and secondary regions, evidenced by an upward flow from the upward-angled primary lobes to the secondary lobes directly above and a corresponding downward flow from the downward-angled secondary lobes to the primary lobes directly below. This process is evident even at short (2.5 cm.) distances from the lobe trailing edge (Fig. 10) and becomes more evident at a distance of 7.5 cm. (Fig. 11). Testimony to the existence of the streamwise vortices, centered on the vertical sidewalls of the lobe mixers, is found in Fig. 11.

The visual data acquired on videotape were analyzed on a video monitor. Measurement of tracings of the dye envelopes displayed on the monitor were used to calculate the above parameters. Photographs are shown in Fig. 12 of videotape records of the dye envelopes occurring at a distance of 15 cm. from the rearward-facing step produced by injecting dye into the flow upstream from the lobe mixers. The laser sheet was positioned normal to the flow. The first photograph shows the dispersion of pink dye injected at a point 30 cm. upstream from the secondary lobe trailing edge. The second photograph shows the dispersion of green dye injected at 10 cm. upstream from the primary lobe. In the third photograph, the interaction occurring when both injection sites are active is shown.

Photographs from videotape of the flowfield observed from the side of the test section are presented in Fig. 13. The trajectory of dye introduced into the secondary flowfield is shown in the leftmost photograph. The result of injecting a green dye into the primary flow field is shown in the other photograph in Fig. 13.

Five of the fourteen configurations examined in the flow visualization experiments were selected as being of most interest for combustion testing, on the basis of the magnitude of the parameters, H_{max}/H_L and $H_{max}/L_{1/2}$, calculated for both the primary and secondary mixers. Configurations that exhibited limited interaction between the primary and secondary flows generally were characterized by values of H_{max}/H_L, based on the secondary lobe mixer height, less than approximately 2. These experimental arrangements also exhibited values of H_{max}/H_L, based on the secondary flow, less than approximately 0.5. The configurations considered for combustion investigations comprised Baseline 2/Alternates 4 and 7, Baselines 4 and 5, and Baseline 4/ Alternate 1.

COMBUSTION TESTS

Combustion tests were performed in a water-cooled test section at pressures on the order of 6 atm. The test section comprises part of a test apparatus that was designed and constructed in a separate effort; features significant to this program are described below and a further description is given in Appendix A. During the combustion experiments, air, heated to a temperature of 500 to 800K was delivered to the test section; the fuel employed was Jet-A. Lobe mixer arrangements evolved from the flow visualization experiments were installed at the upstream end of the test section in close proximity to a 2.5-cm. tall rearward-facing step. Combustion data acquired using these mixers were compared with similar data obtained during baseline shear-layer combustion experiments. Direct observation and gas sampling were used to characterize the effects of the mixer-induced vorticity on the combustion flowfield structure and composition.

EXPERIMENTAL APPARATUS

The water-cooled test section comprises a square duct measuring approximately 15.2 x 15.2 cm. in cross-section and approximately 78.7-cm. long. The sidewalls and upper wall of the test section incorporate water-cooled quartz windows that are approximately 12.7-cm. high and 30.48-cm. long. A flow-preparation section, incorporating flow splitter plates and accommodation for mounting of the linear and convoluted mixer configurations, as well as a fuel injector, immediately precedes the test section, as shown in the schematic diagram comprising Fig. 14. The flow-preparation section is uncooled.

Different splitter-plates may be installed in either the lower (primary) or upper (secondary) locations and the height of each splitter plate may be adjusted between tests. The location of the splitters and the rearward-facing step was selected to enable viewing of the trailing edges of these components during the experiments. The total distance from the exit of the flow straighteners to the rearward-facing step is approximately 54 cm. The secondary/primary splitter terminates at a distance of approximately 44 cm. downstream from the flow straightener exit. The total viewing distance (from the left edge of the left window to the right edge of the right window is approximately 63 cm. A 14-cm. wide area between the two windows includes the window frames and joining flanges. A close-up view of the test

section with a single lobe mixer installed in the lower (primary) airflow path is shown in Fig. 15. The mixer is installed adjacent to the 2.5-cm. high rearward-facing step that is intended to provide a flame stabilization site.

TEST CONFIGURATIONS

Initial experiments comprised acquiring videotaped images of the flame shapes developed through combustion using a linear splitter and convoluted splitters (lobe mixers). The linear splitter was installed in lieu of the primary lobe mixer shown in Figs. 14 and 15. Additionally, no secondary mixer was installed. An original objective comprised acquiring experimental data under conditions simulating gas turbine operation employing a fuel-rich primary zone. The targeted overall fuel-air equivalence ratio was 0.3 and primary-to-secondary air weight flow ratios of 1 and 0.25 were of principal interest. Thus, for each mixer configuration, two air weight flow rate "splits" were used. It was also desired to introduce the primary and secondary airflows in such a way that no significant pressure gradient between the primary and secondary flows would exist at the test section entrance. To accomplish this, an orifice plate was installed in the flow-preparation section to balance the primary and secondary pressure drops.

Based on the experience gained during the test apparatus shakedown test period, conducted as part of a separate effort, and on the extent of the test matrix envisioned for each configuration, it was decided that the combustion evaluation should be focused on a baseline configuration employing no mixing augmentation and two of the five candidates identified in the flow visualization testing. The lobed mixer arrangements selected for testing were Configurations Baseline 4 and Baseline 4/Alternate 1. Schematic diagrams of these two convoluted splitter arrangements are displayed in Fig. 16.

INSTRUMENTATION AND CONTROL

Conventional Instrumentation

Conventional instrumentation including venturies, turbine flow-meters, mass flowmeters, pressure gauges and thermocouples were used to monitor and control the primary and secondary airflows and the fuel flow. The total air weight flow rate was determined using a critical flow venturi positioned upstream from the 720 kW air heater. The primary air weight flow rate was also determined using a critical flow venturi located between the primary flow shutoff valve and the test section. In both venturies, both the total and throat pressures and the air total temperature were measured. Jet-A fuel weight flow rate was measured with a Micromotion C-12 mass flow meter. Coolant flow rates were assessed through the use of paddlewheel flowmeters.

Flow Visualization

Videotaped records of the flame shapes developed during combustion were made by viewing through the side windows of the test section. A circular window in a pipe section situated downstream from the test section afforded a supplementary view, looking upstream, of the combustion region. The latter view was provided by a stationary Panasonic VHS format video camera. The views from the side of the test section were provided by a remotely controlled VHS format video camera which could be aimed at either of the two test section windows. The camera focal length and aperture could be varied

from a controller situated in the test cell control room.

Emission Gas Sampling

Gaseous emissions data were acquired through the aid of a rake equipped with seven aerodynamically quenching sampling probes (Ref. 7,8). A schematic diagram of one of the probes is provided in Fig. 17. Theoretically, under conditions of sufficiently great total pressure, the flow entering the probe at the entrance orifice is critical and expands to a supersonic Mach number within the divergent internal passage shown. A shock wave system is established at the sudden expansion, providing partial recovery of the total pressure. The supersonic expansion, augmented by active cooling of the probe, results in a rapid decrease in static temperature that tends to quench all further chemical reaction. It is of course, mandatory that the total pressure remain sufficiently high to permit delivery of the sample to the gas analysis equipment.

The seven probes in the rake were situated laterally, when viewed from a downstream location (Fig. 18). One probe was positioned centrally with respect to the duct and the lobe mixer. Three probes were located axially downstream from the lobe vertical sidewalls and the remaining three probes were situated midway between the sidewalls. Surveys were generally made at five vertical positions above the lower surface of the test section duct, corresponding nominally to the vertical locations shown in the figure. The surveys were performed at one axial location, viz., 27.3 cm. from the edge of the rearward-facing step, as shown in Fig. 14. This distance was selected because it was assumed that much of the effect of the convoluted splitters on the flowfield would have been completed at that distance and relatively high combustion efficiency levels would be developed.

Additional descriptive material relating to the emissions sampling instrumentation is provided in Appendix B.

Test Conditions

The primary parameters that were varied in the experimental program were the mixer configuration, the velocities of the primary and secondary flows, and the fuel flow rate. The Jet-A fuel was delivered only to the lower half of the primary airflow. This extremely rich fuel-air mixture was then combined, through the action of the primary lobed mixer, with the flow in the upper half of the primary stream to form the mixture that was consumed in the combustor primary zone. The range of the flow conditions established for the combustion tests is displayed in Table III.

Test Procedures

The test procedure comprised the following basic steps:

1. Establish total airflow through heater and test apparatus.
2. Initiate coolant flows to test apparatus.
3. Initiate flow of current to electric air heater.
4. Monitor test section entrance temperature while adjusting power to heater.
5. Upon attaining desired temperature, initiate fuel injection and ignition sequence.

6. Subsequent to ignition of fuel, adjust pressure in test section using backpressure valve in exhaust duct.

During the performance of experiments to provide visual records of the flame shape, the following subsequent steps were taken:

7. Record, on videotape, the flame image appearing in the port-side upstream and downstream windows using the remotely operated video camera.

8. Record, on videotape, the flame image appearing in the window at the exit of the test section.

9. Using the data acquisition system, record the flow conditions corresponding to flame image data.

10. Vary the flow rate of fuel delivered to the test section.

11. Adjust the test section backpressure as required.

12. Repeat steps 7 through 11, until blowoff occurs or until stable combustion is no longer observed.

13. Terminate all flows subsequent to "cooldown" period.

During the experiments involving emissions sampling, the following procedure, subsequent to step 6, above was pursued:

7. With the sampling rake at its initial position, initiate flow to the gas analysis system through the first probe.

8. Acquire emissions data and record the concomitant test section flow conditions, using the data acquisition system.

9. Purge the first probe and initiate flow through the second probe.

10. Repeat this sequence until data have been acquired using the seven probes in the sampling rake.

11. Relocate the rake to a second selected height above the test section floor.

12. Repeat steps 7 through 12 until data have been acquired for five vertical positions of the rake.

13. Terminate all flows subsequent to "cooldown" period.

Test Results

Testing was carried out in two phases. The first series of experiments were conducted to record the flame envelopes that were developed by the linear and convoluted splitter plates relative to the initial velocity levels and the fuel-air equivalence ratios during combustion of the fuel. In the second series of tests, emissions sampling data were acquired using a seven-probe rake positioned horizontally at a distance of 27.3-cm downstream from the trailing edge of the rearward-facing step. The rake was traversed vertically across the flow during combustion of the fuel at an overall equivalence ratio of approximately 0.3.

Flame Envelope Visualization

The results of the tests to document the extent of flame spreading achieved with the different splitter plates and

different flow conditions are presented as photographs of the flame envelopes recorded on videotape in VHS format. Photographs of the recorded flame envelopes for each of the configurations examined, acquired during combustion at an overall equivalence ratio of 0.3, are shown in Figs. 19 through 21. At the left edge of these figures, the marks indicate, from bottom to top respectively, the positions of the rearward-facing step, the primary splitter plate and the secondary splitter plate.

The flame patterns produced by the linear splitter plate are shown in Fig. 19. At the top in the figure are shown the flame envelopes appearing in the upstream and downstream port-side windows when the primary-to-secondary weight flow rate ratio, $W_p/W_s = 0.20$. Corresponding photo-graphs for $W_p/W_s = 0.84$ are shown at the bottom of the figure.

In Fig. 20, the flames produced by the convoluted splitter, Baseline 4 are shown. At the top are the envelopes for $W_p/W_s = 0.27$ and at the bottom are the corresponding flame envelopes for $W_p/W_s = 0.74$. Even a cursory comparison between these flame envelopes and those shown in the previous figure for the linear splitter reveals the rapid upward turning of the flow induced by the presence of the lobed mixers. (The irregularly shaped dark regions in the photographs comprise deposits of soot on the cooled windows.)

Similar results were obtained during experiments with the convoluted splitter, Baseline 4/Alternate 1, the results of which are shown in Fig. 21. Again, the flame envelopes shown at the top in the Figure comprise those recorded for a weight flow rate ratio, $W_p/W_s = 0.27$ while those at the bottom are for $W_p/W_s = 0.75$.

It was indicated previously that a second video camera was used to provide images of the combustion region as viewed from a circular window located downstream from the test section (Fig. 14). A typical videotaped image acquired from this vantage point is shown in Fig. 22. (The circular object in the foreground is the support yoke used to provide vertical motion of the sampling rake.) At high fuel-air ratios, the image of the flame fills the frame. The figure shows an image acquired at a fuel-air ratio of approximately 0.017. The lobed mixer used is B4 (Baseline 4) and the primary-to-secondary air weight flow ratio, $W_p/W_s = 0.27$. Note the similarity between this flame geometry and the shapes of the dye traces shown in Fig. 12, acquired during the water flow visualization experiments. The "tongues" or "fingers" of flame, separated by darker, unfueled regions occur immediately downstream from the "upward-turning" lobes. The recorded images show that this flame structure persists even at the lowest fuel-air ratios examined.

Gaseous Emissions Data

Gaseous emissions data were acquired for each of the two lobed mixer configurations, B4 and B4A1. In these experiments, the overall fuel-air equivalence ratio was maintained at a constant level of approximately 0.3 while the seven-probe rake was traversed vertically through the combustion zone at a distance of 27.3 cm. downstream from the trailing edge of the rearward-facing step.

Gas samples were analyzed to yield oxygen (O_2), nitric oxides (NO), carbon monoxide (CO), carbon dioxide (CO_2), and unburned hydrocarbon (UHC) concentrations. Using the procedure outlined by Spindt in Ref. 9, the local fuel-air ratios were calculated from the measured concentration data. The data

plotted in Figs. 23 and 24 display the fuel-air ratios determined at each probe location as the height of the rake above the test section floor, H was varied. The data in Fig. 23 are for the mixer configuration, B4. Owing to the formation of soot during initial tests with the rake, no more than five of the seven probes were available for this investigation. For the data of Fig. 23, the overall fuel-air ratio was 0.020 and the primary-to-secondary air weight flow ratio, $W_p/W_s = 0.70$. Difficulties encountered with the operation of the rake traversing mechanism required that two separate tests be performed to acquire the data for the mixer configuration, B4A1. The data acquired from these two tests are presented in Figs. 24a and 24b. The overall fuel-air ratio for the two tests was 0.022 and $W_p/W_s = 0.3$.

DISCUSSION OF RESULTS

WATER FLOW VISUALIZATION

Intense, large-scale vortices were formed in water flow visualization experiments using single convoluted splitter plates. These streamwise vortices were developed even when no significant velocity ratio existed between the upper (secondary) and lower (primary) streams initially segregated by the flat splitter plate preceding the convoluted (lobed) mixer.

For cases where the convoluted splitter was installed adjacent to the rearward-facing step that produced a flame-stabilization site in close proximity to the splitter, an interaction between the vortex flowfield and the step-induced recirculation zone occurred when the trailing edge of the splitter was placed upstream from the step. This interaction was indicated by a decrease in the length of the recirculation zone. The air bubble tracks revealed the presence of between three and four separate vortex structures existing within the recirculation zone induced by the flow over the rearward-facing step. The length of the recirculation zone, in general, was between 5 and 7 step heights, consistent with the data reported by other investigators (10,11) for a similar Reynolds number range.

Of the fourteen configurations involving primary and secondary mixer lobe combinations, five enhanced-mixing configurations were identified that were characterized by strong interactions between the primary and secondary flows. The interactions induced a substantial vertical interchange of primary and secondary fluid, resulting in intermingling of the two fluids covering up to 80 percent of the duct height in distances from the lobe mixer trailing edges ranging from approximately 8.1 to 16.5 cm., i.e., from approximately one-half to one duct height. All of these arrangements involved positioning the two splitters so that their lobes were "in phase" with one another. That is, the peaks of the primary mixer lobes were adjacent to valleys of the secondary mixer lobes and all lobes were aligned with one another. When the lobes of the mixers were positioned to be "out of phase" with one another, no mixing of the primary and secondary was observed to occur.

It was observed that overlap or "nesting" of the lobes yielded the strongest interactions and merging of the primary and secondary flows. No merging of the vortices developed by the two flows was observed when a linear splitter plate extended to the trailing edges of the convoluted splitter. To attain strong interaction and merging, the maximum permissible separation between the primary and secondary lobes, measured according to the parallel tangents through the respective lobe peaks, appears to be approximately 5 mm.

HIGH-PRESSURE COMBUSTION

The results of the combustion tests indicated that convoluted splitter configurations which, in water flow visualization experiments, developed large-scale vortex structures, would do so in the combustion environment. The configurations examined exhibited significant primary/ secondary flow interactions, e.g. local merging of the flow fields owing to the interactions between the primary and secondary vortices, and displacement of each of these flows by the other.

The impact of the lobed mixers on the flow was to induce a rapid interchange of fluid between the primary and secondary flow regions, causing most of the fuel, which was introduced into the primary flow near the lower surface of the test section, to be transferred to the upper part of the test section flowfield. All of this occurred in approximately two duct heights, measured from the trailing edge of the primary-flow lobed mixer. The objective of this research effort was to determine whether improvements, relative for example, to the heat release rate and combustor-exit temperature profile exhibited in shear-layer combustion, could be obtained through the application of streamwise vorticity. The results of this investigation do demonstrate an approach to large-scale manipulation of the flow field geometry.

Line drawings of the flame envelopes for some of the configurations examined are included in Appendix C. These line drawings were prepared from the videotape records and provide a chronological sequence showing the variation in the area covered by the flame envelope. The line drawings were also used as the basis for defining the flame front angles. It was found that, at distances downstream from the rearward-facing step greater than approximately two duct heights, the measured inclination of the flame front for the convoluted splitter plates examined was essentially the same as that of the linear splitter. That is, at that distance, the forced-mixing induced by the presence of the lobed mixers is no longer effective. The redistribution of fuel and air has essentially been completed and conventional shear-layer mixing, driven by the available turbulent energy, proceeds.

Variations in the inclination of the flame front related to the fuel-air equivalence ratio were calculated based on the measurements of the flame shapes recorded on videotape. Flame angles, α_1 through α_5 are defined in the diagram shown in Fig. 25. The dramatic effect that the lobed mixers have on the flame angles is demonstrated by the data shown in Figs. 26 through 28. In Figure 26, the effect of fuel-air ratio variations on the flame angles induced using the linear splitter are shown for primary-to-secondary air weight flow rate ratios, W_p/W_s of approximately 0.2 and 0.7. For the lower primary air weight flow rate (Fig. 26a), the variation of the flame angle is not substantial, increasing to no more than approximately four degrees at the highest fuel-air ratio examined. When W_p/W_s is increased from the lower value of 0.2 to 0.7 (Fig. 26b), the flame region was observed to expand and the flame angles essentially doubled over the range of fuel-air ratios developed. In both cases, the flame angles increased gradually as the fuel-air ratio was increased. The sudden variation occurring at a fuel-air ratio of approximately 0.0135 corresponds to an abrupt relocation of the point to which the leading edge of the flame was "anchored", viz., from the trailing edge of the step to the trailing edge of the splitter.

A similar relationship between fuel-air ratio and flame angle accrued when the lobed mixers replaced the linear splitter.

However, the flame angles developed substantially exceeded those associated with the linear splitter, increasing to levels of approximately 17 degrees at the highest fuel-air ratios imposed. These data are shown in Figs. 27 and 28 for the B4 and B4A1 lobed mixer configurations, respectively. Note, in Fig. 27, that at the downstream locations, where α_3 and α_4 were measured, the flame angles have decreased to the levels associated with free shear-layer combustion, i.e., on the order of 5 degrees.

The measured fuel-air ratio data acquired at several heights above the floor of the test section have been recast and plotted in Figs. 29 and 30 which depict the measured fuel-air ratio distributions relative to the height above the lower surface of the test section. All of the fuel delivered to the test apparatus was injected into the primary airflow which was introduced within the lower 7.5 cm. of the test section. The impact of the lobed mixers on the flow is to induce a rapid interchange of the primary and secondary flow regions, causing most of the fuel-air mixture to be transferred to the upper part of the test section flowfield. The configuration, B4A1, in which the trailing edges of the convoluted splitters were aligned, appears to be more effective in carrying out this process. The configuration, B4, in which the upper lobed mixer trailing edge was displaced 5 cm. downstream with respect to the lower mixer trailing edge, appears to delay this interchange. Additional surveys at distances greater than and less than 27.3 cm from a step could aid in validating this hypothesis.

To furnish a check of the fuel-air ratio data, the arithmetic average values of the measured fuel-air ratios were compared with the mass flow ratio of Jet-A fuel and air introduced to the experiment during the emissions sampling tests. The data of Fig. 29 yield an average fuel-air ratio of 0.019 compared with the direct measurement of 0.020. Similarly, the data of Fig. 30 yield an average fuel-air ratio of 0.021 compared with a direct measurement based on measured flow rates of 0.022. The agreement between the averaged data based on sampling measurements and the values based on measured flow rates lends credence to the validity of the fuel-air ratio measurements that quantify the dramatic exchange of fluid from the lower portion of the duct to the upper portion.

Combustion efficiencies were calculated from the measured gaseous emissions of carbon monoxide, CO and unburned hydrocarbons, UHC. Based on the following expression (see Ref. 12) the inefficiency was determined,

$$1-\eta=\frac{(EI)_{CO}(Q_L)+(EI)_{UHC}(Q_L)_{fuel}}{(Q_L)_{fuel}\ x\ 1000}$$

where η = Combustion efficiency at probe location

$(EI)_i$ = Emissions index in gm./kg. fuel for ith gas species

$(Q_L)_i$ = Lower heating value for gas species, i in cal./gm.

The emissions index for species, i is given by the equation,

$$(EI)_i = X_i \frac{M_i}{M} \frac{1+f/a}{f/a}\ x\ 10^3$$

where X_i = Mole fraction of species, i

M_i = Molecular weight of species, i

M = Average molecular weight of combustion products

f/a = Fuel-air ratio of the gas sample.

The calculated combustion efficiencies for the convoluted splitters are shown in Figs. 31 and 32, relative to the location at which the sample data were recorded. The levels registered for the Baseline 4 configuration, evaluated with a level of the primary-to-secondary air weight flow ratio, W_{prf}/W_{sec} = 0.70, are high. The values shown range from approximately 98.3 to 99.98 percent, implying that a relatively high degree of mixing of the fuel and air was achieved in the region between the fuel injection site and the sampling location. On the other hand, combustion efficiency levels recorded for the other convoluted splitter, configuration Baseline 4/Alt. 1, shown in Fig. 32, range downward from approximately 99.9 percent to approximately 81.3 percent. This configuration was evaluated using a level of W_{prf}/W_{sec} = 0.3. Conceivably, the mixing of the fuel and air was not as readily accomplished using this reduced primary-to-secondary air weight flow ratio.

Because all of the fuel was delivered into only one-half of the primary airflow, when a flow rate ratio, W_{prf}/W_{sec} = 0.3, was used, the equivalence ratio in the fueled part of the primary flow was approximately 2.6. When a level of W_{prf}/W_{sec} of 0.7 was used, the equivalence ratio of the fueled part of the primary flow was decreased to approximately 1.4. The differences in combustion efficiency levels can, therefore, be attributed either to differences in the primary-airflow ratio, W_{prf}/W_{sec} or to the differences in the two splitter configurations.

CONCLUSIONS

WATER FLOW VISUALIZATION

- Intense, large-scale vortices are formed with single, convoluted splitter plates even when no significant velocity ratio exists.

- Strong primary/secondary flow interactions may be developed using dual convoluted splitters, that induce a substantial vertical interchange of primary and secondary fluid to occur. This can result in the intermingling of the two fluids covering up to 80 percent of the duct height in distances from the lobed mixer trailing edges ranging from approximately one-half to one duct height.

- Whether or not these strong interactions, which result in merging of the primary and secondary flows, occur is related to the proximity of the secondary streamwise vortices with respect to the primary streamwise vortices.

HIGH-PRESSURE COMBUSTION

- Convoluted splitter configurations which, in water flow visualization experiments, induce the development of large-scale vortical structures, will, for comparable Reynolds numbers, develop these structures in a combustion environment.

- The projections or "fingers" of flame, observed from a vantage point downstream from the combustion region, are formed as a consequence of the primary-secondary vortex interaction, independent of the extent of heat release.

- The inclination of the flame front developed during combustion experiments with the lobed mixers was on the order of three times that developed when a linear splitter plate was used. The effects of the vortical structures on flame spreading are greatest in the region within two duct heights or six lobe heights of the splitter trailing edge, both values being consistent with the results cited in Ref. 6.

- Low pressure-loss lobed mixer configurations can effectively promote large-scale mass exchange between primary and secondary flows when the relative mass flow rates are of the order found in gas turbine main burners. Further work would be required to determine if mixer designs which utilize the full pressure drop available can provide the rapid breakdown to the small scale required for combustion.

RECOMMENDATIONS

- Based on the combustion test results, a reexamination of the water flow visualization experiments, using two convoluted splitters should be focused on evaluating approaches to enhancing mixing of the primary and secondary streams on the molecular level while retaining the large-scale benefits accrued through the introduction of streamwise vorticity. Logical candidate strategies involve manipulation of the lobed-mixer trailing edge, e.g. small-scale vortex generation or the use of scalloped trailing edges. A quantitative assessment of the mixing potential of a configuration should be conducted utilizing image analysis techniques.

- In the combustion experiment, attention should be directed toward acquiring additional information regarding the spatial (axial and vertical) variation in the fuel-air distributions for the splitter configurations examined. Additionally, the effects of the primary-zone stoichiometry and the placement of the fuel admitted to the primary zone should be evaluated to assess their impact on the inferred combustion efficiencies.

ACKNOWLEDGEMENTS

The experimental studies were supported under the U.S. Army Research Office Contract DAAL03-89-C-0018. The ARO Project Officer was David M. Mann. Technical coordination was provided by George Bobula, U.S. Army Propulsion Directorate, Cleveland, Ohio. Funding was provided in part by the National Aeronautics and Space Administration, Lewis Research Center, Cleveland, Ohio. NASA activities were coordinated by James D. Holdeman and Edward J. Mularz. The test apparatuses were provided by the United Technologies Research Center.

The flow visualization studies were carried out with the assistance of David Holcomb. The combustion studies were performed with the assistance of J. L. Grimes. The photographic and video imaging activities were supported by Robert J. Haas.

REFERENCES

1. McVey, J. and J. Kennedy: Flame Propagation Enhancement Through Streamwise Vorticity Stirring, AIAA Paper 89-0619 (1989).

2. McVey, John B.: Accelerated Combustion Through Streamwise Vorticity Stirring, UTRC Report 88-38, August, 1988.

3. Paterson, R. W.: Turbofan Mixer Nozzle Flow Field - A Benchmark Experimental Study. Journal of Engineering for Gas Turbines and Power, Vol. 106 (1984).

4. Presz, W., R. Gousy and B. Morin: Forced Mixer Lobes in Ejector Designs, AIAA Paper 86-1614 (1986).

5. Skebe, S. A., R. W. Paterson and T. J. Barber: Experimental Investigation of Three-Dimensional Forced Mixer Lobe Flow Fields, AIAA Paper 88-3785, July 1988.

6. McCormick, D. C.: Vortical and Turbulent Structure of Planar and Lobed Mixer Free-Shear Layers, Ph.D. Thesis, University of Connecticut, 1992.

7. Chiappetta, L. and M. B. Colket, III: Design Considerations for Aerodynamically Quenching Gas Sampling Probes, Jnl. of Heat Transfer, Vol. 106, May, 1984, pp. 460-466.

8. Colket, III, M. B., L. Chiappetta, R. N. Guile, M. F. Zabielski, and D. J. Seery: Internal Aerodynamics of Gas Sampling Probes, in Measurements; Diagnostics, Combustion and Flame, 44:3-14 (1982).

9. Spindt, R. S.: Air-Fuel Ratios from Exhaust Gas Analysis, SAE Paper 650507, Mid-Year Meeting, Chicago, IL, May 17-21, 1965.

10. Krall, K. M. and E. M. Sparrow: Turbulent Heat Transfer in the Separated, Reattached and Redevelopment Regions of a Circular Tube, Jnl. of Heat Transfer, ASME Trans., V.88, February, 1966, pp. 131-136.

11. Runchal, A. K.: Mass Transfer Investigation in Turbulent Flow Down-Schmidt Numbers, International Jnl. of Heat and Mass Transfer, Vol. 14, 1971, pp. 781-791.

12. Blazowski, W. S., R. E. Henderson: A Review of Turbopropulsion Combustion, Part I, Fundamentals of Combustion, AFAPL-TR-77-41, June, 1977.

TABLE I

GEOMETRIC CHARACTERISTICS OF LOBED MIXER CONFIGURATIONS

Splitter Config'n.	H_{1p} cm.	H_{1s} cm.	X_{1p} cm.	X_{1s} cm.	α_p deg	α_s deg	H_{st} cm.	h_{st} cm.	X_{sp} cm.
Baseline 1	5.33	-	0	-	0	0	2.54	-	0
Baseline 1/ Alternate 1	5.33	-	5.08	-	0	0	2.54	-	0
Baseline 1/ Alternate 2	5.33	-	-5.08	-	0	0	2.54	-	-5.08
Baseline 2	5.33	3.56	0	0	0	0	2.54	0	0
Baseline 2/ Alternate 3	5.33	3.56	0	5.08	0	-5.7	2.54	0.64	-10.16
Baseline 2/ Alternate 4	5.33	3.56	0	5.08	0	0	2.54	0.64	-10.16
Baseline 2/ Alternate 5	5.33	3.56	0	-5.08	0	0	2.54	0.64	-10.16
Baseline 2/ Alternate 6	5.33	3.56	0	-5.08	0	-3.8	2.54	0.64	-10.16
Baseline 2/ Alternate 7	5.33	3.56	0	5.08	0	-9.0	2.54	0.64	-10.16
C-1	5.33	3.56	0	5.08	0	-5.6	2.54	0.64	-10.16
Baseline 3	5.33	3.56	0	0	0	0	2.54	0	0
Baseline 4	3.56	5.33	0	5.08	2.5	0	3.81	0	-10.16
Baseline 4/ Alternate 1	3.56	5.33	0	0	2.5	0	3.81	0	-10.16
Baseline 5	3.56	5.33	0	0	6.1	0	3.81	0	-10.16

TABLE II
SUMMARY OF FLOW VISUALIZATION DATA

CONFIG.	RUN NO.	Upri/ Usec	Re per foot x 10^-5 primary upper	primary lower	secondary	Usec ft/sec.	PRI. LRZ/ HST	L 1/2 pri. in.	L 1/2 sec. in.	Hmax/Hlp pri.	Hmax/Hls sec.	Hmax. pri. in.	Hmax. sec. in.	Hmax/ L 1/2 pri.	Hmax/ L 1/2 sec.	Lpri in.	Lsec in.
B/L 1	27	15.50	1.00	2.50	0.17	0.20	8.00	7.0		1.90	na	3.99	0.00	0.57	na	7.96	na
		10.00	1.80	1.70	0.17	0.20											
	thru	7.00	2.40	1.10	0.17	0.20											
		2.00	1.10	2.80	0.17	0.20											
	37	20.00	1.30	3.40	0.17	0.20											
	60-62	10.00	1.70	1.70	0.17	0.21											
B1 Alt1	51-59	15.50	1.00	2.80	0.17	0.20	7.50	8.0	4.90	1.90	na	3.99	0.00	0.50	na	5.96	na
		10.50	1.90	1.70	0.17	0.20											
		7.00	2.40	1.10	0.17	0.20											
	67	3.80	1.80	1.50	0.38	0.50											
	68	1.30	1.20	1.10	0.82	1.00											
B1 Alt2	38-47	15.50	1.00	2.80	0.17	0.20	8.90	8.7	5.50	1.80	na	3.76	0.00	0.43	na	6.00	na
	48-50	1.80	1.10	2.90	0.17	0.20											
	69	3.80	1.80	1.50	0.41	0.50											
	70	1.30	1.20	1.10	0.79	1.00											
B/L 2	71-73	3.80	1.50	1.50	0.38	0.50	6.00	6.0	4.60	1.90	1.50	3.99	2.10	0.67	0.46	5.12	5.25
	74	1.80	1.10	1.10	0.75	0.90											
	75	1.00	1.20	1.20	1.23	1.50											
	76-77	0.50	0.80	0.80	1.66	2.00											
	78	0.50	0.80	0.80	1.66	2.00											
	79,81	1.00	0.01	1.60	1.66	2.00											
	80,82	0.02	1.60	0.03	1.66	2.00											
B/L 3	83	1.80	0.90	0.90	0.52	0.63	7.00	7.0	5.00	2.00	1.60	4.20	2.24	0.60	0.45	6.00	6.05
		2.30	1.20	1.20	0.52	0.63											
	84	5.10	1.80	1.50	0.28	0.35											
	85	3.20	1.80	1.50	0.47	0.57											
	86	1.40	1.20	1.10	0.75	0.91											
B2 Alt3	89-94	0.70	1.80	0.85	1.20	1.40	8.00	8.0	5.00	2.50	1.80	5.25	2.66	0.66	0.53	7.39	7.60
C-1	95	0.70	1.80	0.85	1.20	1.40	8.00	8.0	5.50	2.50	2.00	5.25	2.80	0.66	0.51	8.75	7.00
	96	1.70	0.70	2.00	1.20	1.40											
	97-99	0.70	1.80	0.85	1.20	1.40											
B2 Alt4	100-102	0.70	1.80	0.85	1.10	1.30	7.00	8.3	4.50	2.50	2.10	5.25	2.94	0.63	0.65	7.95	7.00
B2 Alt5	103-104	1.70	1.80	0.83	1.10	1.30	7.80	8.0	4.40	1.80	1.70	3.36	2.38	0.56	0.54	8.20	8.21
B2 Alt6	105-108	0.85	1.50	1.00	1.10	1.40	7.00	8.0	7.40	2.30	1.70	4.83	2.38	0.81	0.32	7.92	9.92
B2 Alt7	109	1.00	1.70	1.10	1.20	1.40	8.70	8.0	4.00	2.20	3.80	4.62	5.32	0.58	1.33	9.63	8.82
B/L 4	110	2.80	3.00	3.00	1.10	1.30	5.50	4.0	4.36	3.10	2.30	4.34	4.83	1.09	1.11	9.04	8.80
	111	1.80	2.80	2.80	1.40	1.80											
	112	2.00	3.10	3.10	1.50	1.90											
	113	0.58	1.20	1.20	2.20	2.70											
B4 Alt1	114	2.10	3.30	3.30	1.50	1.90	5.70	4.9	5.70	3.80	2.50	5.32	5.25	1.09	0.92	9.67	9.55
	115	1.90	3.00	3.00	1.80	1.90											
	116	0.24	0.80	0.80	2.40	2.90											
	117	0.24	0.48	0.48	2.00	2.44											
	118	1.21	1.42	1.42	1.18	1.43											
	119	0.44	0.89	0.89	2.00	2.44											
B/L 5	120	1.28	1.51	1.51	1.18	1.44											
	121	1.11	1.55	1.55	1.40	1.71											
	122	0.27	0.53	0.53	1.95	2.38											
	123	1.28	1.55	1.55	1.21	1.48	3.70		3.00	3.10	2.40	4.34	5.04		1.68	8.04	7.88
	124	1.13	1.55	1.55	1.37	1.67	4.00		3.00	4.20	2.50	5.89	5.25		1.75	9.05	7.84
	125	0.23	0.44	0.44	1.97	2.40	4.50		3.00	3.90	2.00	5.46	4.20		1.40	7.98	7.78
	126	1.26	1.55	1.55	1.23	1.50											
	127	1.52	2.57	2.57	1.69	2.06											

TABLE III

SUMMARY OF COMBUSTION TEST CONDITIONS

Splitter Config'n.	Pri. Vel. m'sec	Sec. Vel. m/sec	W_{pri}/W_{sec}	Overall Equiv. Ratio	Primary Equiv. Ratio
Linear	6.1-15.1	15.2-21.3	0.20-0.70	0.06-0.32	0.42-1.81
Baseline 4	6.7-15.8	12.2-17.4	0.26-0.75	0.06-0.35	0.31-1.62
Baseline 4/ Alternate 1	6.1-14.9	11.3-18.0	0.26-0.80	0.06-0.35	0.30-1.62

Total Air Weight Flow Rate, kg/sec.: 0.90-1.07
Test Section Entrance Temperature, K: 506-806

1. For flame visualization experiments, the overall fuel-air equivalence ratio was varied in discrete steps during the combustion test, from approximately 0.3 to a value near lean blowoff.

2. For emissions sampling experiments, the overall fuel-air equivalence ratio was maintained during the entire test at a value of approximately 0.3.

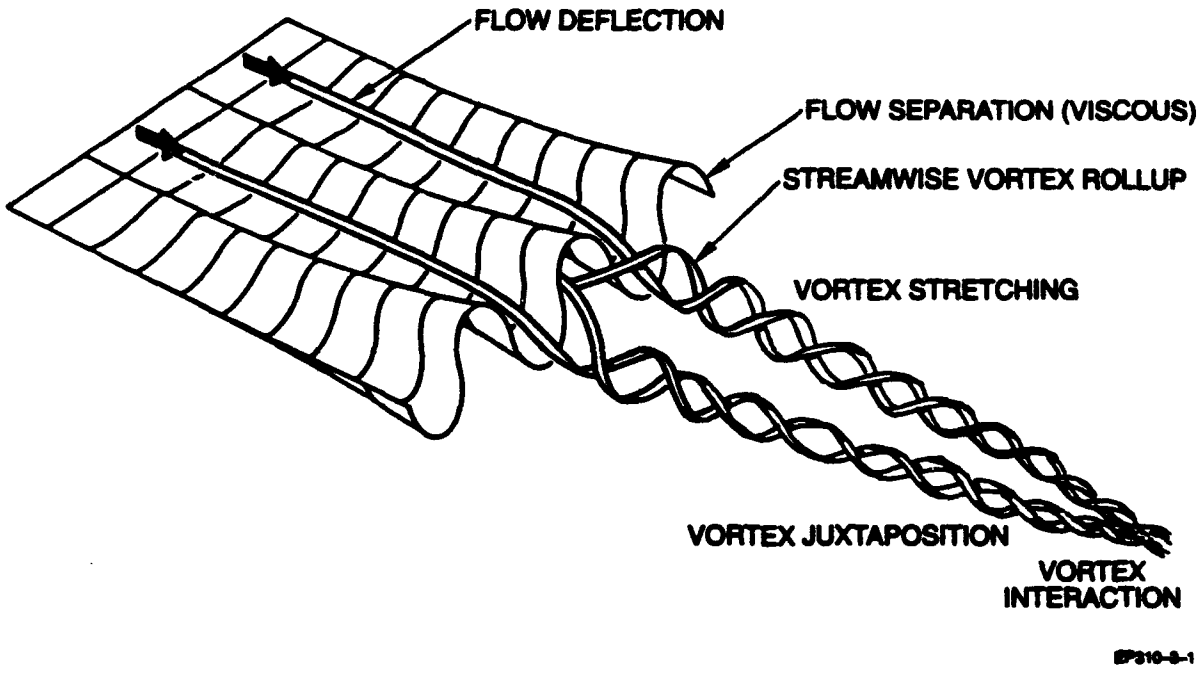

Figure 1. Mixing Enhancement by a Convoluted Flow Splitter

EP310-3-2

Figure 2. Overall View of Flow Visualization Test Apparatus

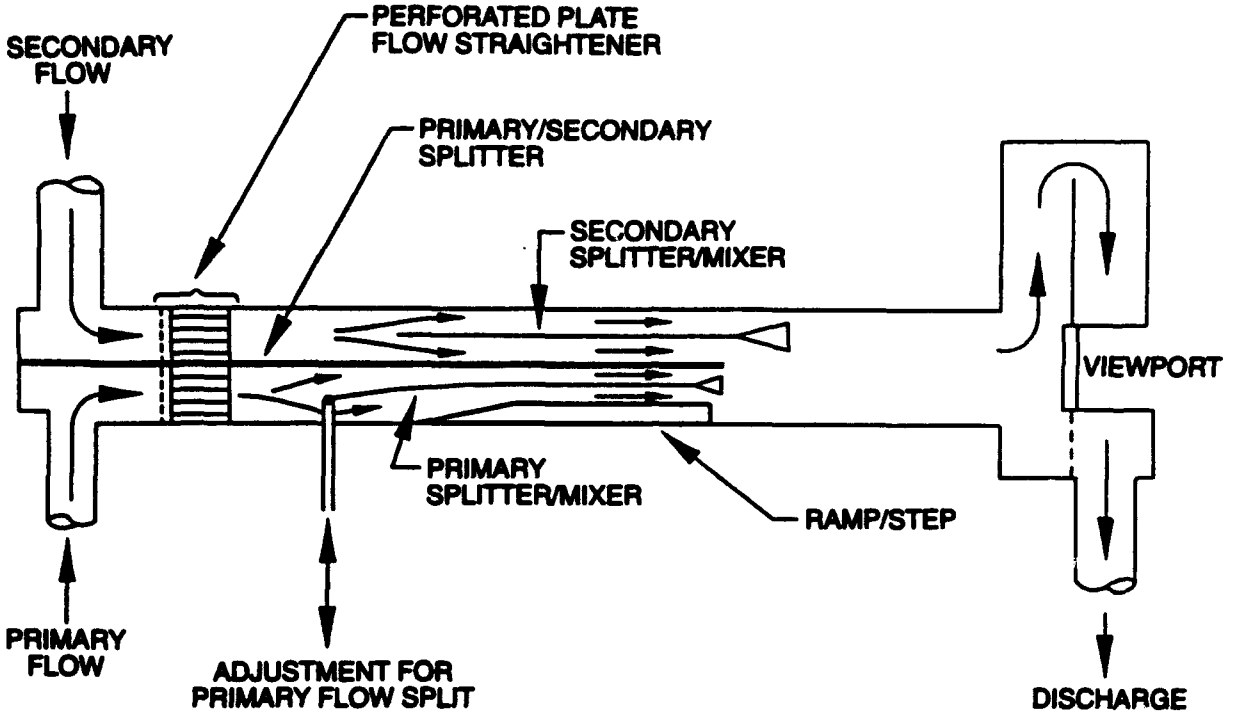

Figure 3. Flow Visualization Test Section

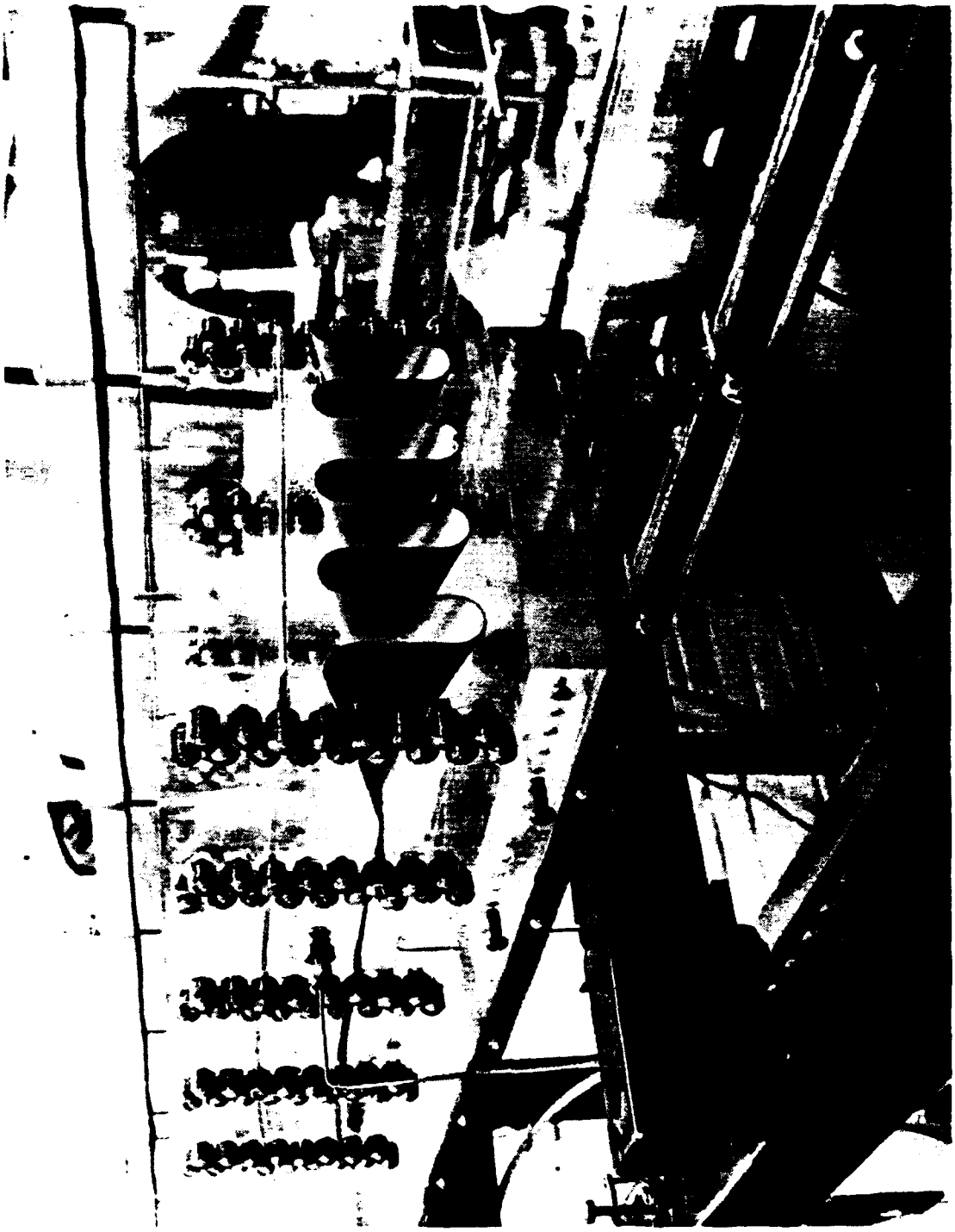

Figure 4. Single Four-Lobe Mixer in Primary Flowpath

EP310-3-4

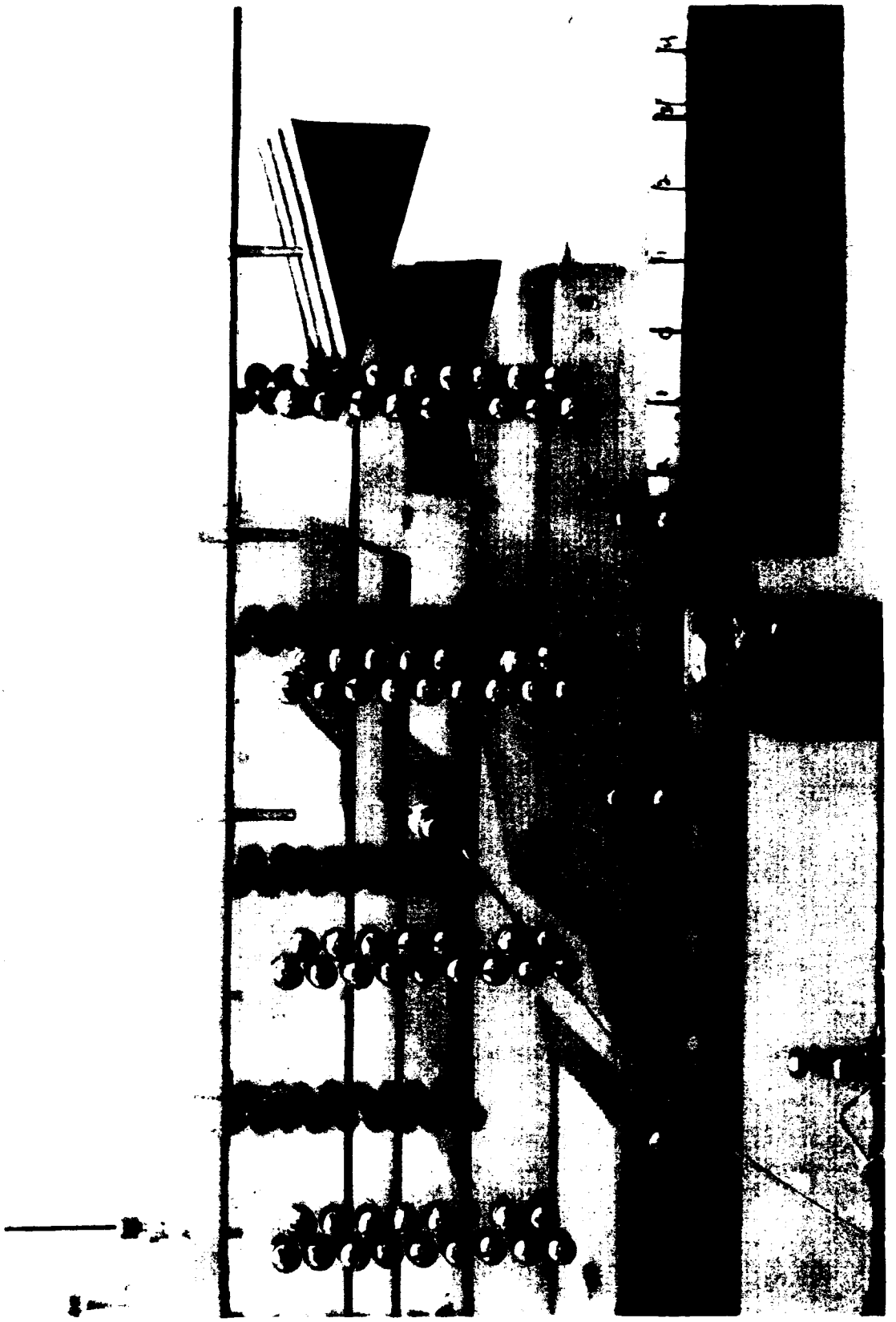

EP310-3-6

Figure 5. Dual Four-Lobe Mixers and Splitter Plates

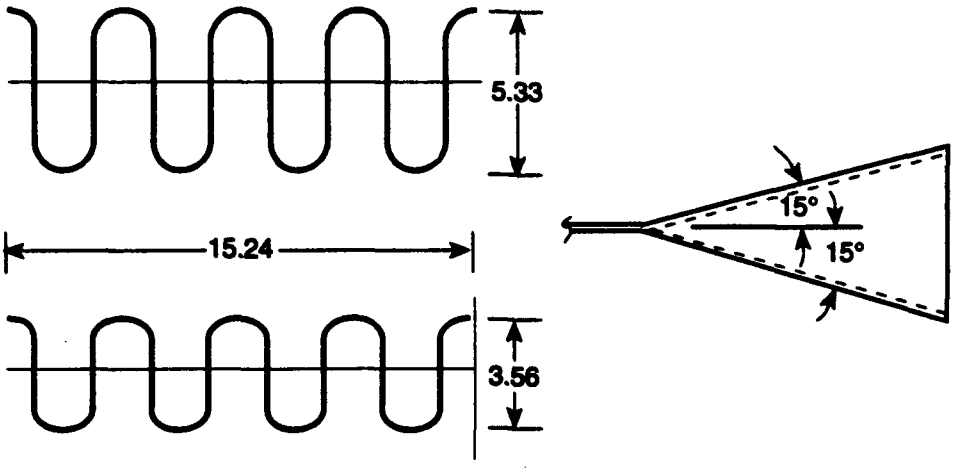

EP310-3-6

Figure 6. Four-Lobe Mixer Dimensions (Penetration = 0.7)

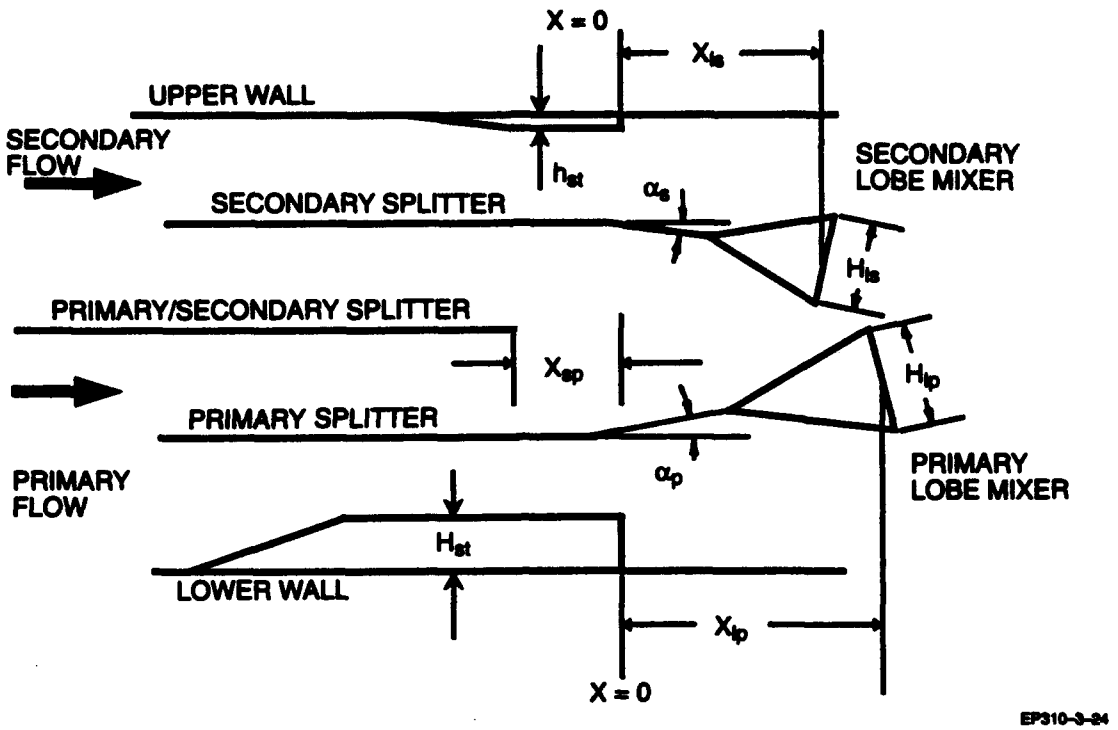

Figure 7. Nomenclature for Lobed Mixer Configurations Used in Flow Visualization Experiments

EP310-3-18

Figure 8. Enhanced-Mixing Configuration Baseline 4

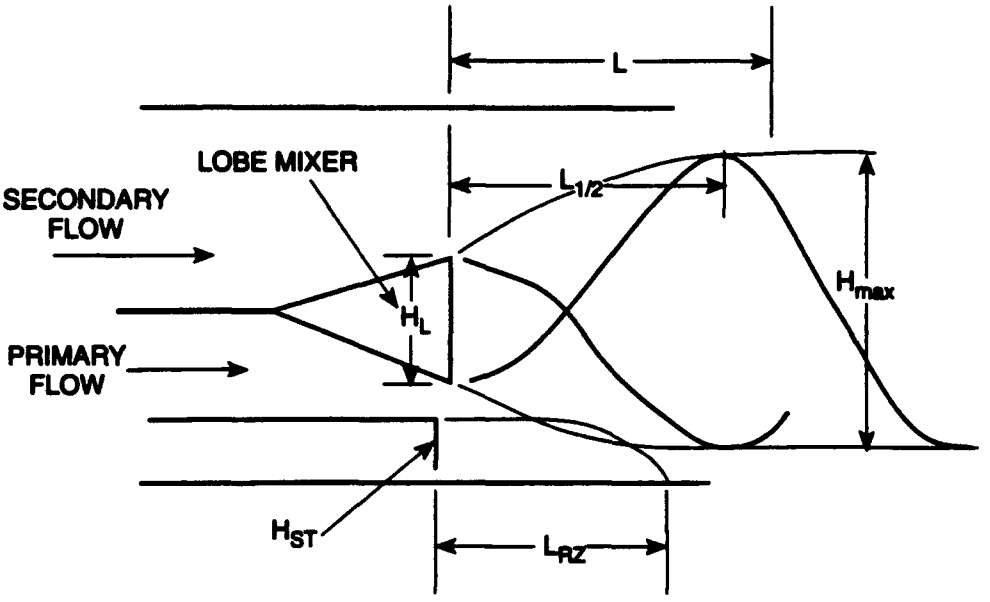

EP310-3-7

Figure 9. Mixer Flowfield Nomenclature

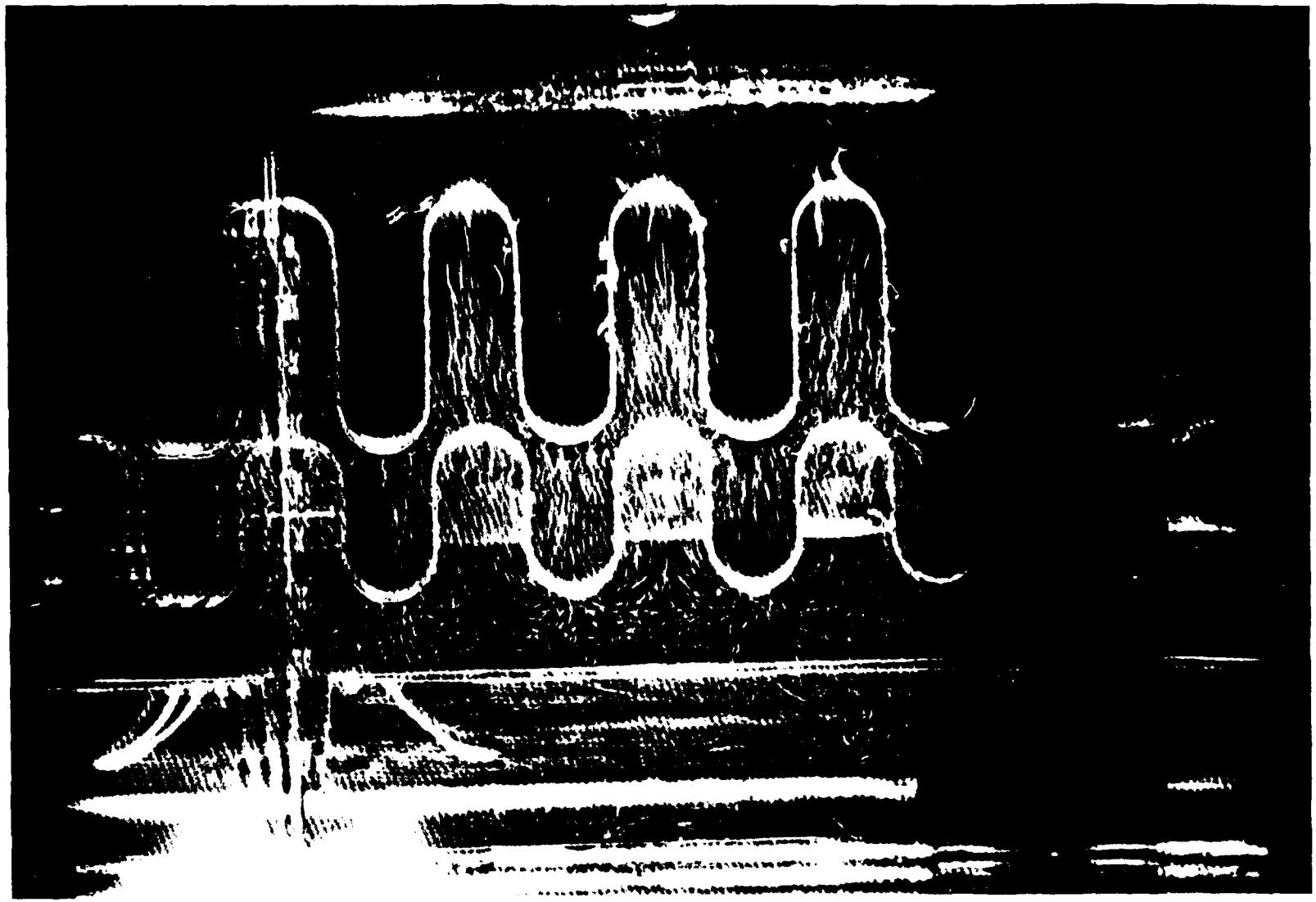

EP310-3-8

Figure 10. Baseline 4/Alt.1 Mixer Flowfield at a Distance of 2.54 cm From Step

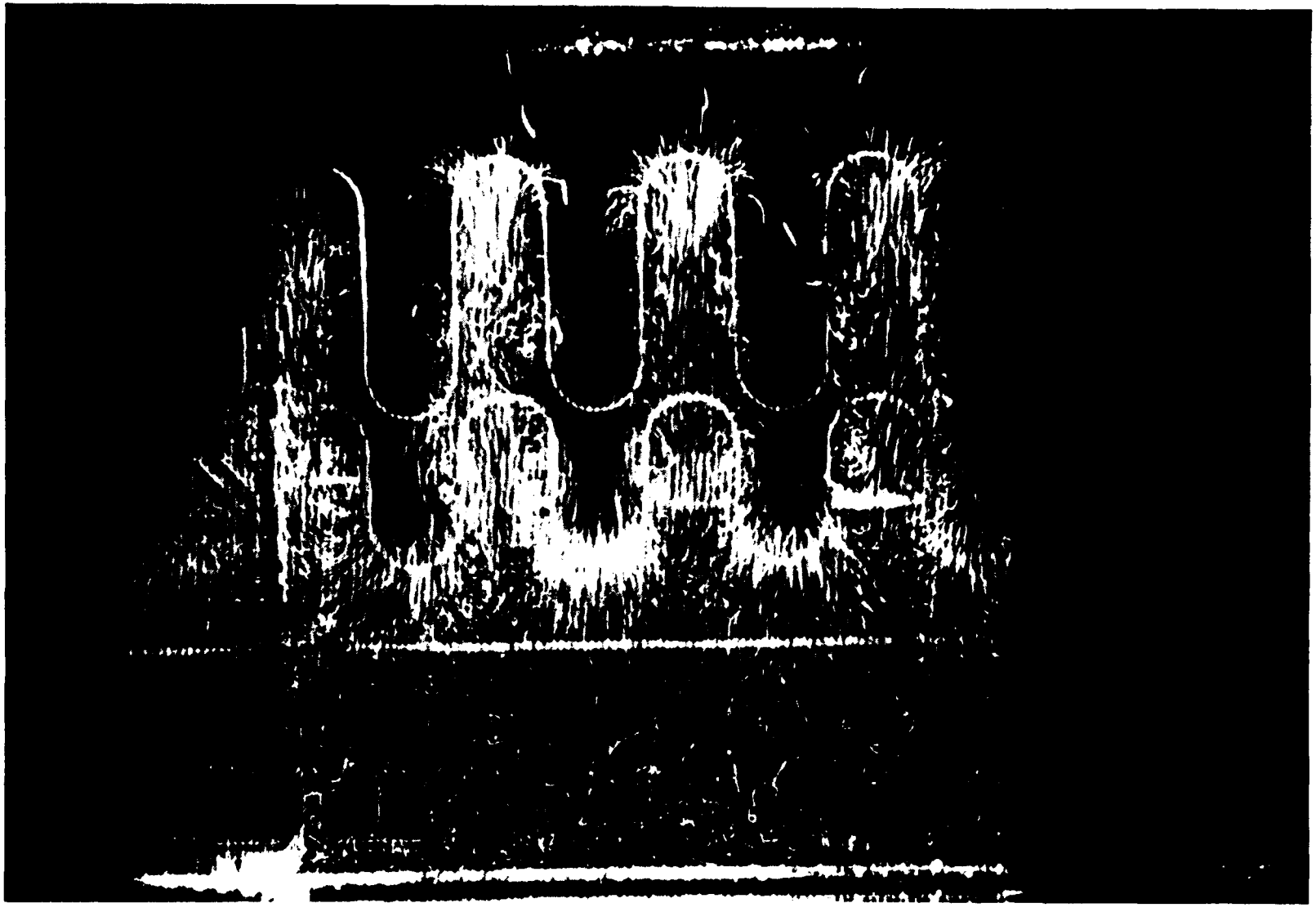

EP310-3-9

Figure 11. Baseline 4/Alt.1 Mixer Flowfield at a Distance of 7.62 cm From Step

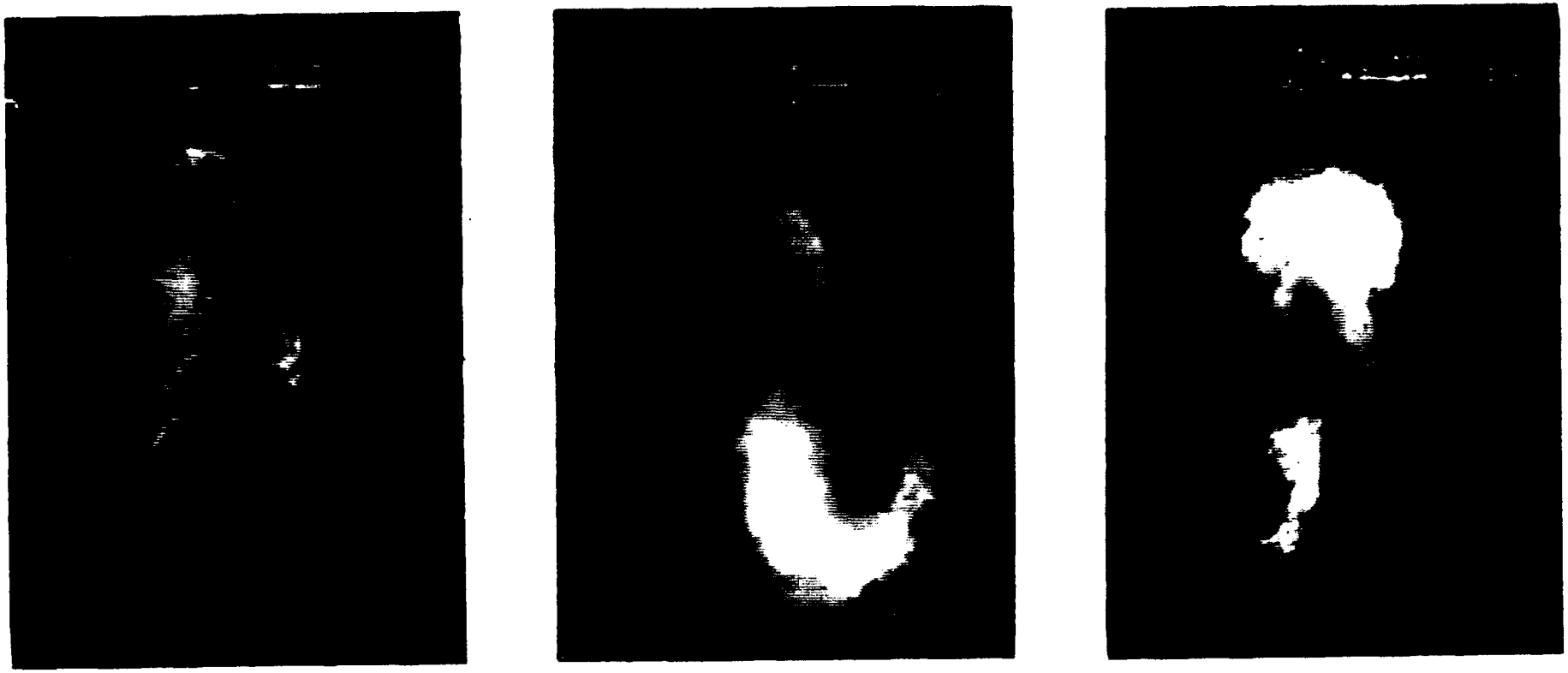

Pink Dye in Secondary

Green Dye in Primary

Dye in Both Streams

Figure 12. End Views of Dye Envelopes at a Distance of 15 cm from Step Configuration Baseline 4

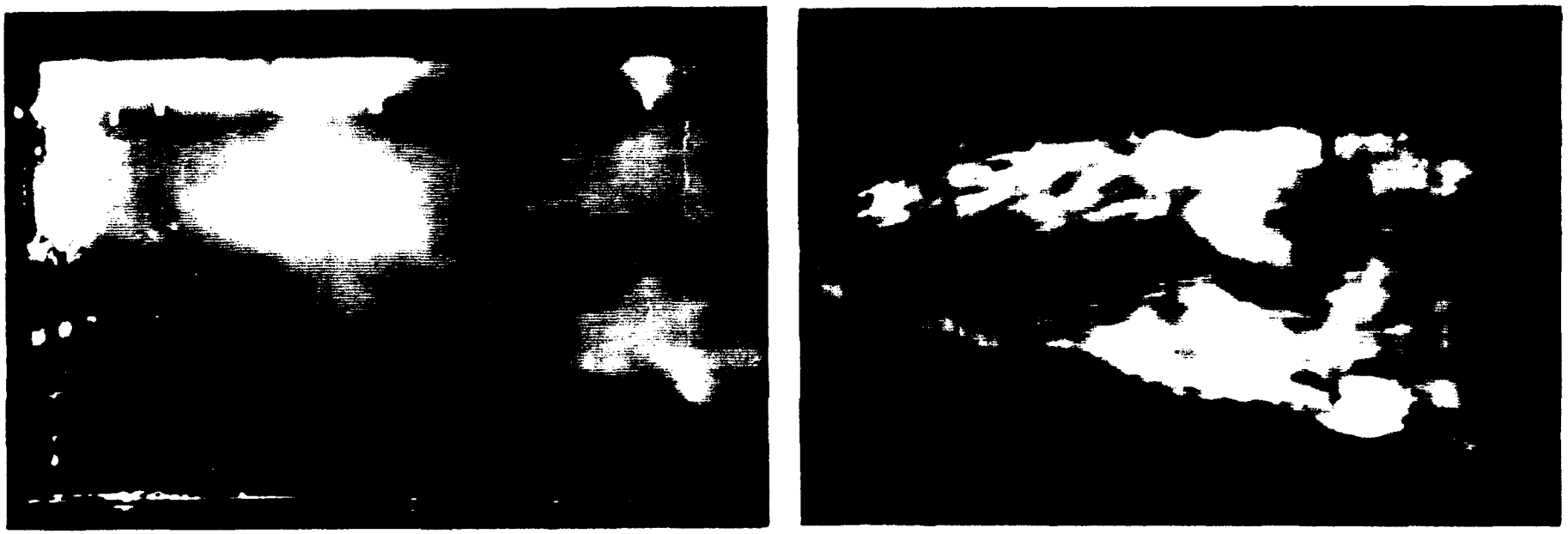

Pink Dye in Secondary

Green Dye in Primary

Figure 13. Side Views of Dye Envelopes. Configuration Baseline 4/Alt. 1

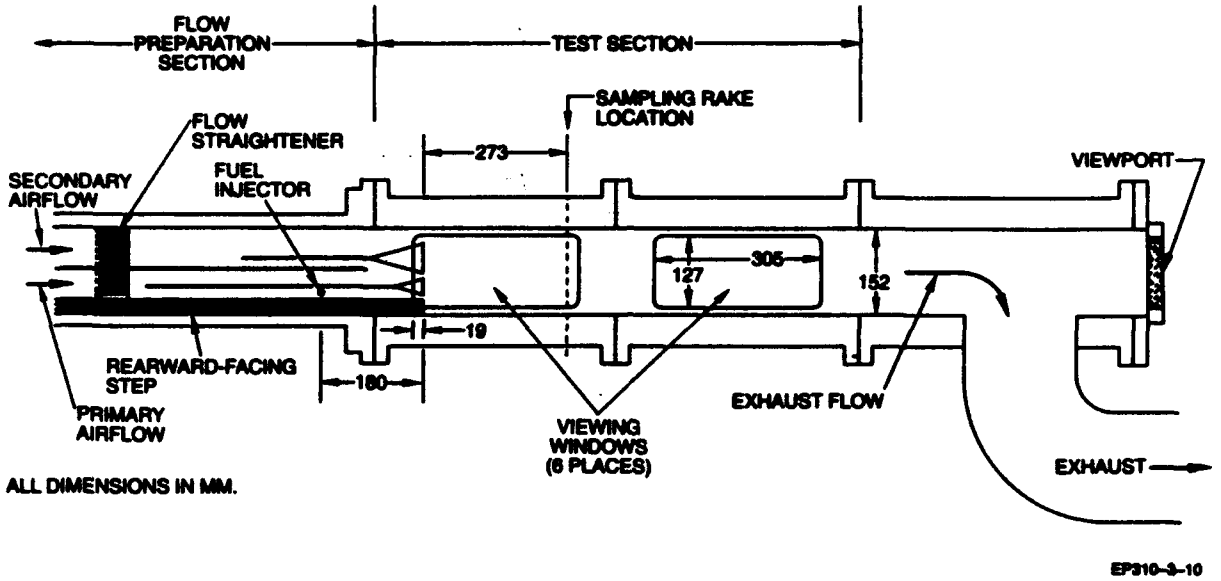

Figure 14. Schematic Diagram of Combustion Test Apparatus

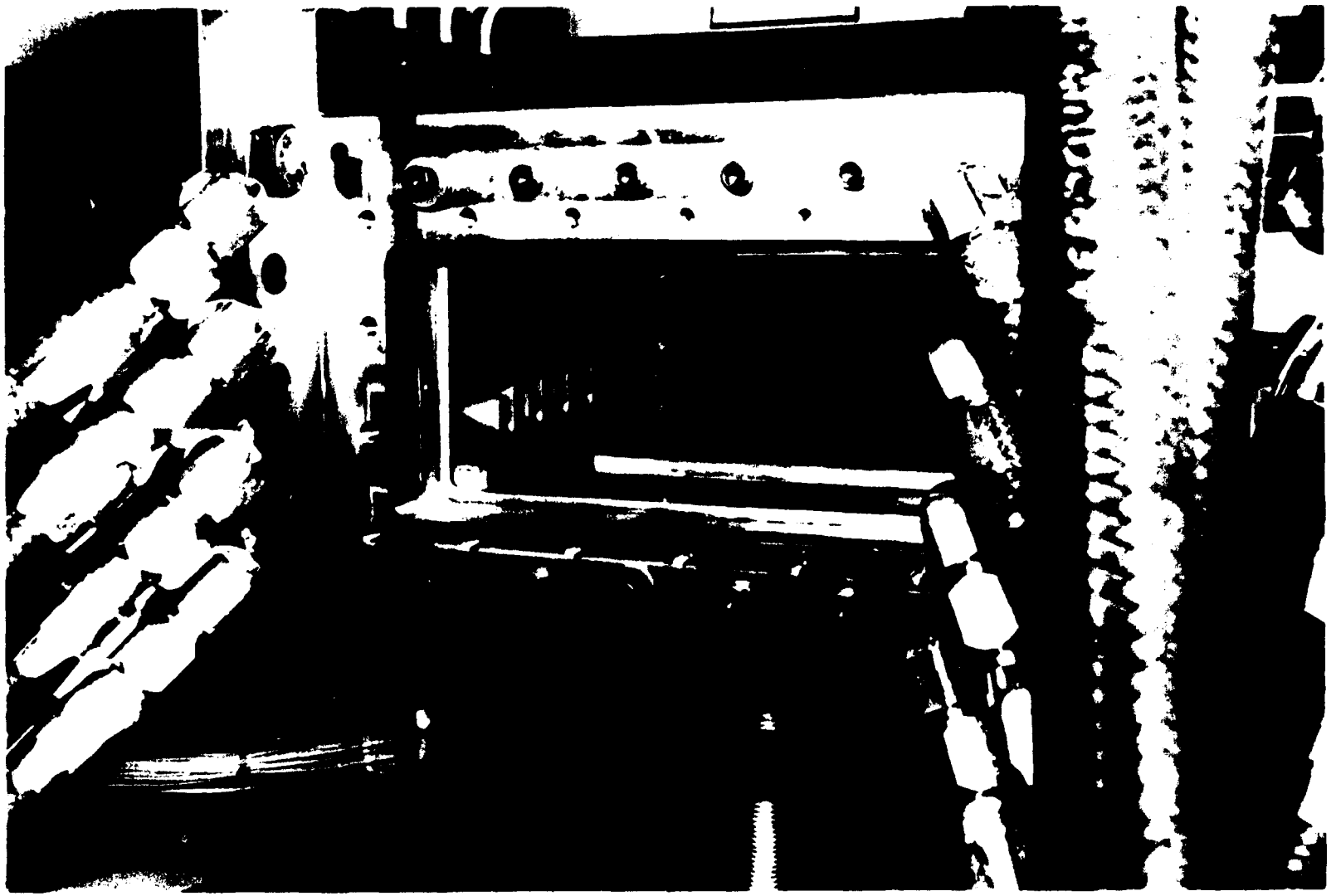

EP310-3-11

Figure 15. Single Four-Lobe Mixer Installed in Combustion Test Section

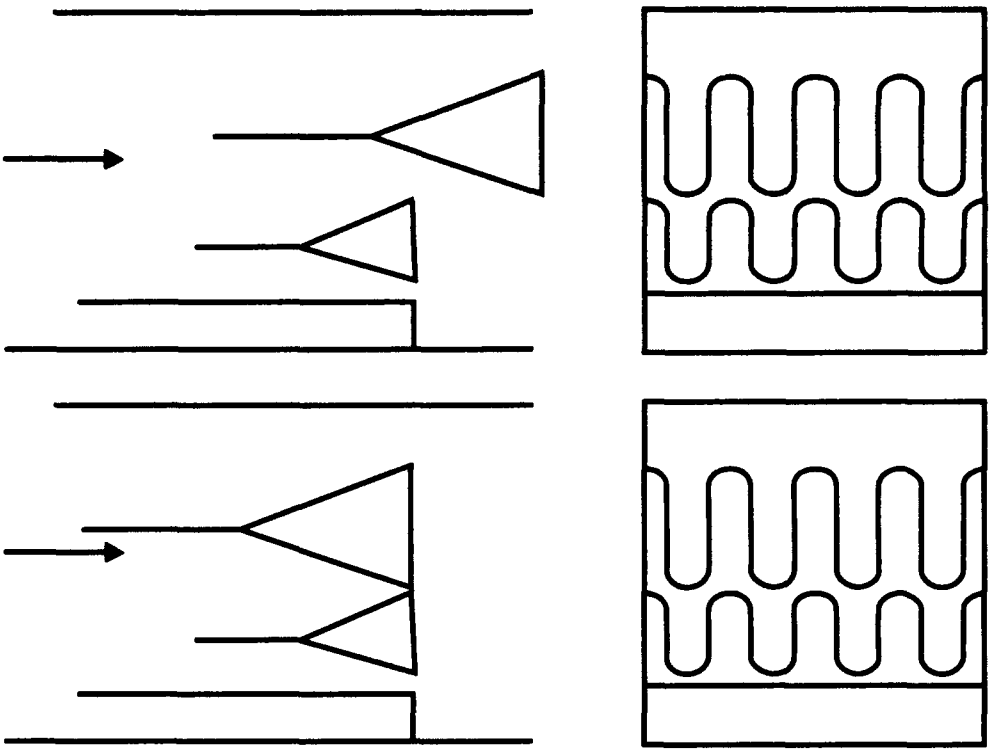

EP310-3-47

Figure 16. Schematic Diagrams of Combustion Test Configurations Baseline 4 (Upper) and Baseline 4 Alternate (Lower) (See Table I for Dimensions)

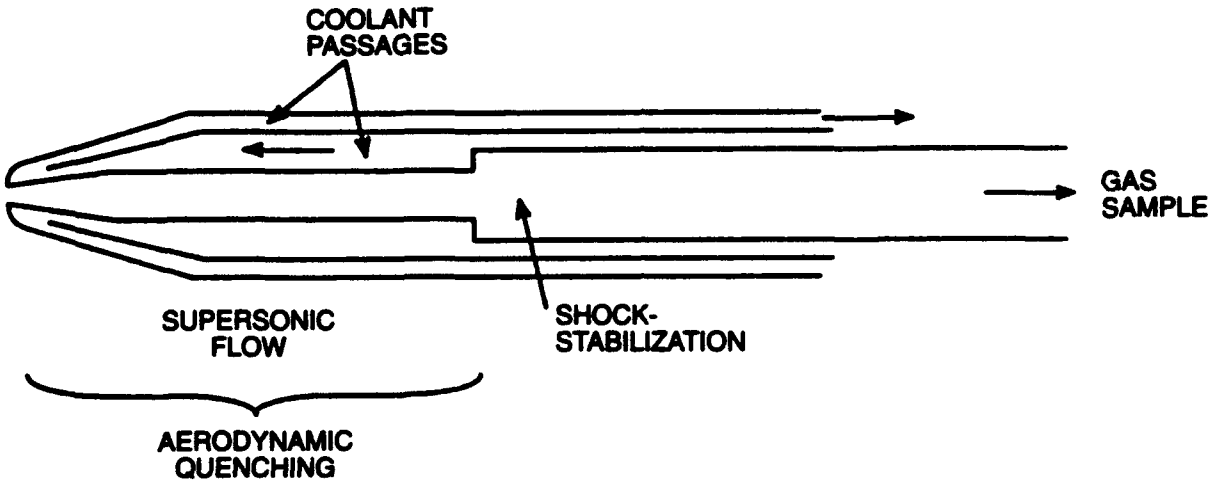

EP310-3-12

Figure 17. Aerodynamically Quenching Probe

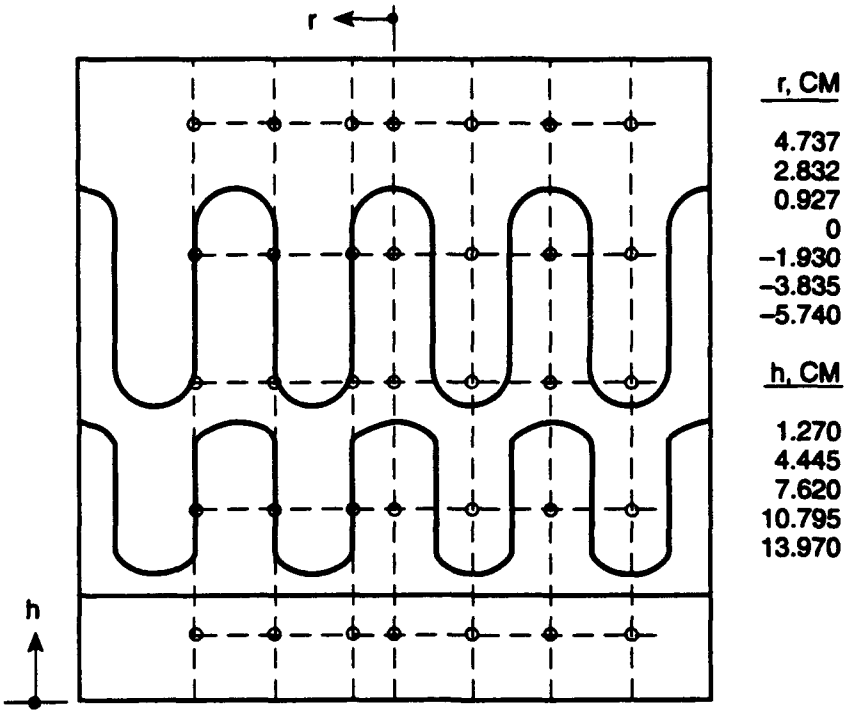

EP310-3-13

Figure 18. Planned Emissions Sampling Locations (View Looking Upstream)

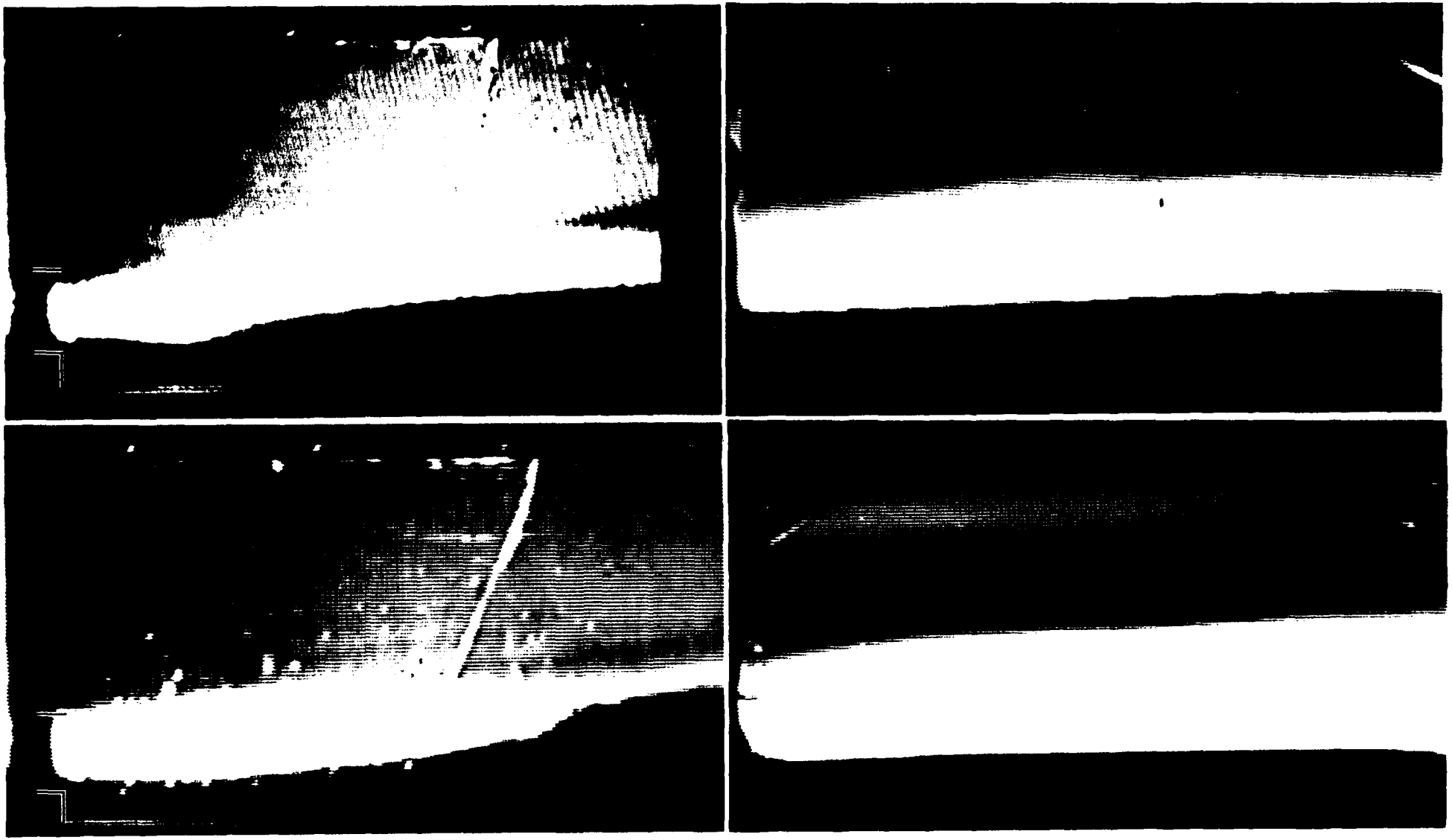

Upstream Window

Downstream Window

Figure 19. Videotaped Images of Flames Developed with Linear Splitter Jet-A Combustion at E.R. = 0.3. Upper W_{pri}/W_{sec} = 0.20 Lower W_{pri}/W_{sec} = 0.84.

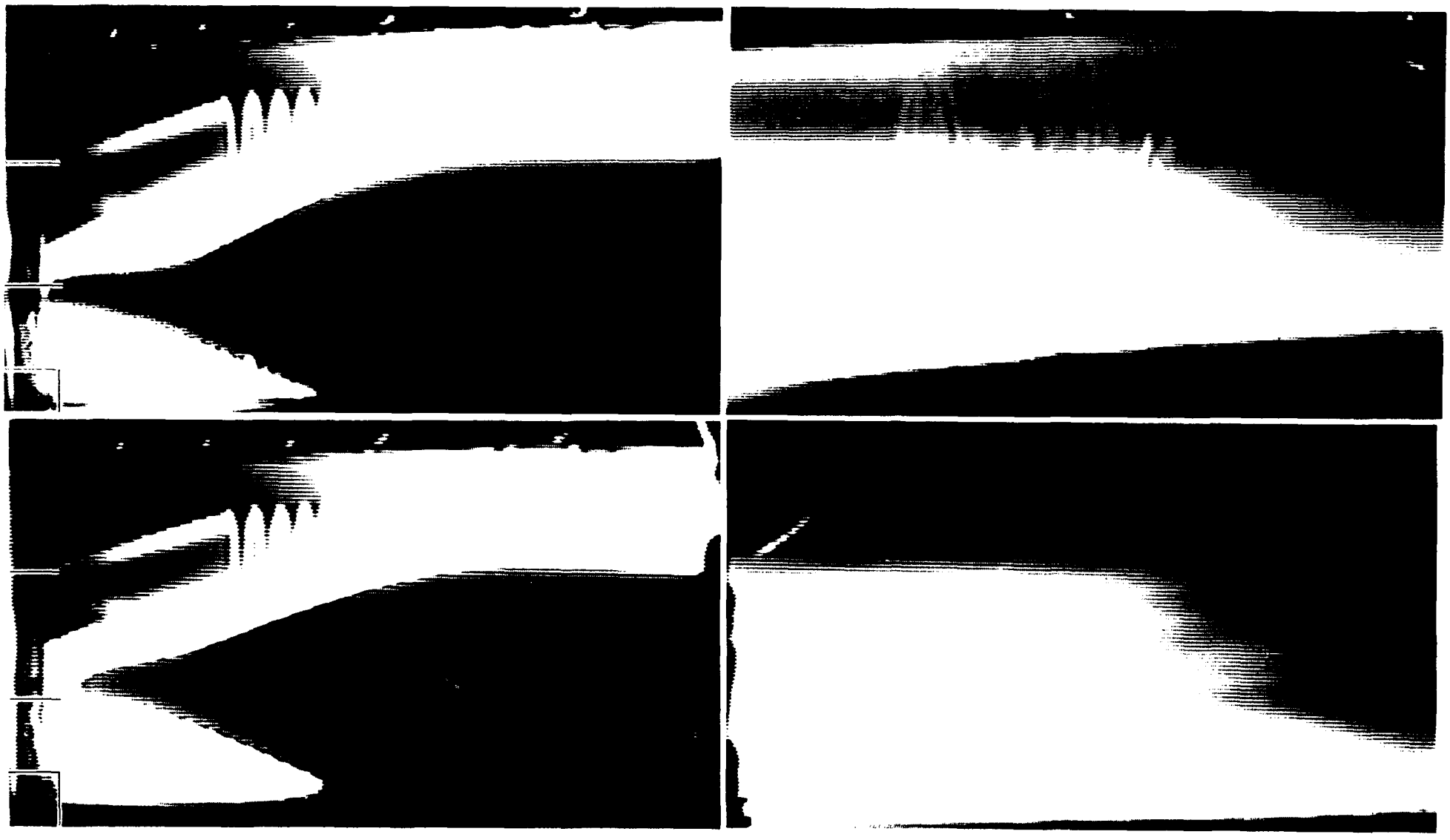

Upstream Window

Downstream Window

Figure 20. Videotaped Images of Flames Developed with Convoluted Splitter, B4. Jet-A Combustion at E.R. = 0.3. Upper Wpri/Wsec = 0.27 Lower Wpri/Wsec = 0.74.

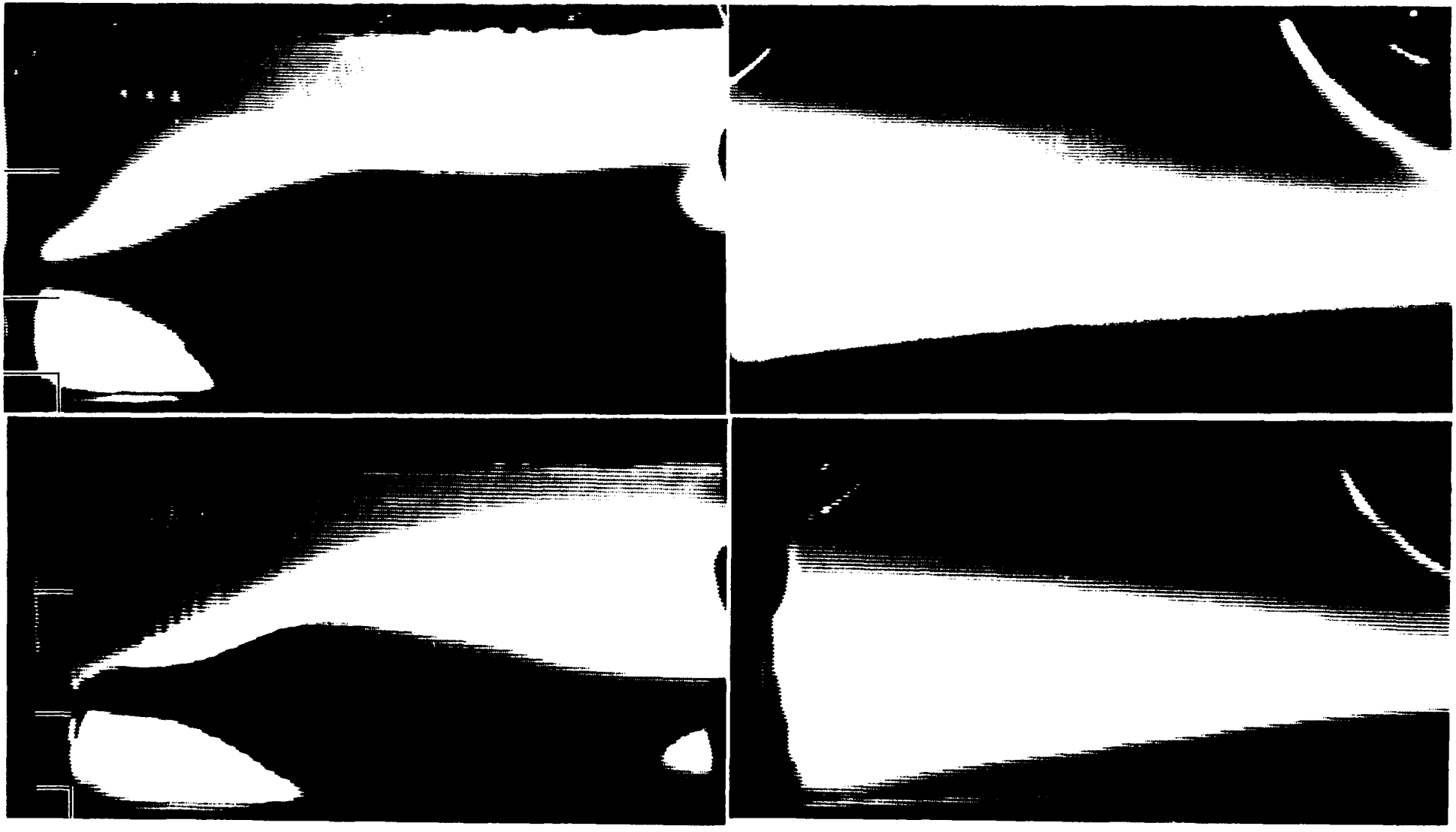

Upstream Window

Downstream Window

Figure 21. Videotaped Images of Flames Developed with Convoluted Splitter, B4A1 Jet-A Combustion at E.R. = 0.3, Upper Wpri/Wsec = 0.27 Lower Wpri/Wsec = 0.75.

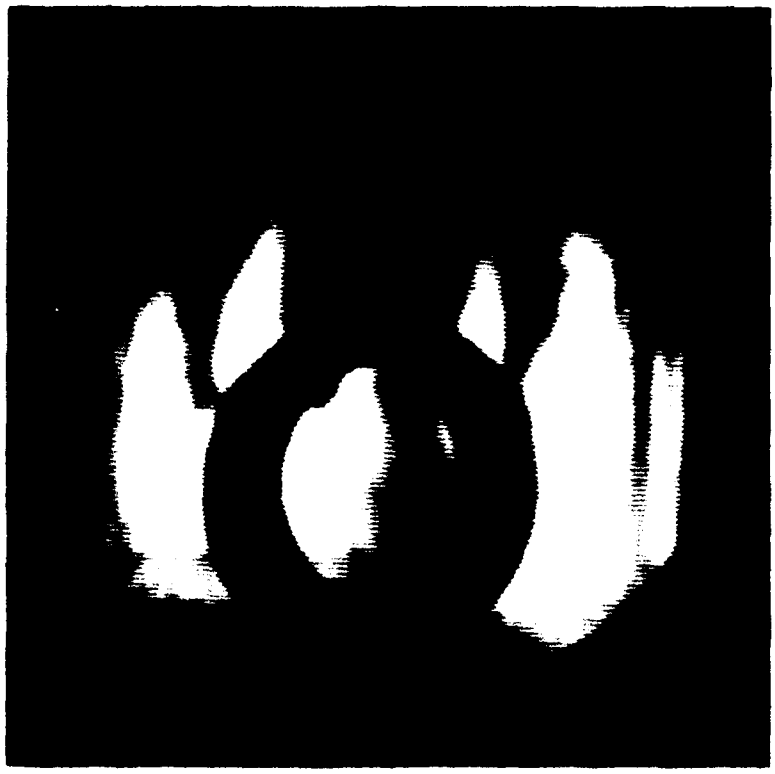

Figure 22. Videotaped Image of Flame Viewed from Downstream Window Convoluted Splitter, B4. Jet-A Combustion at E.R. = 0.24.

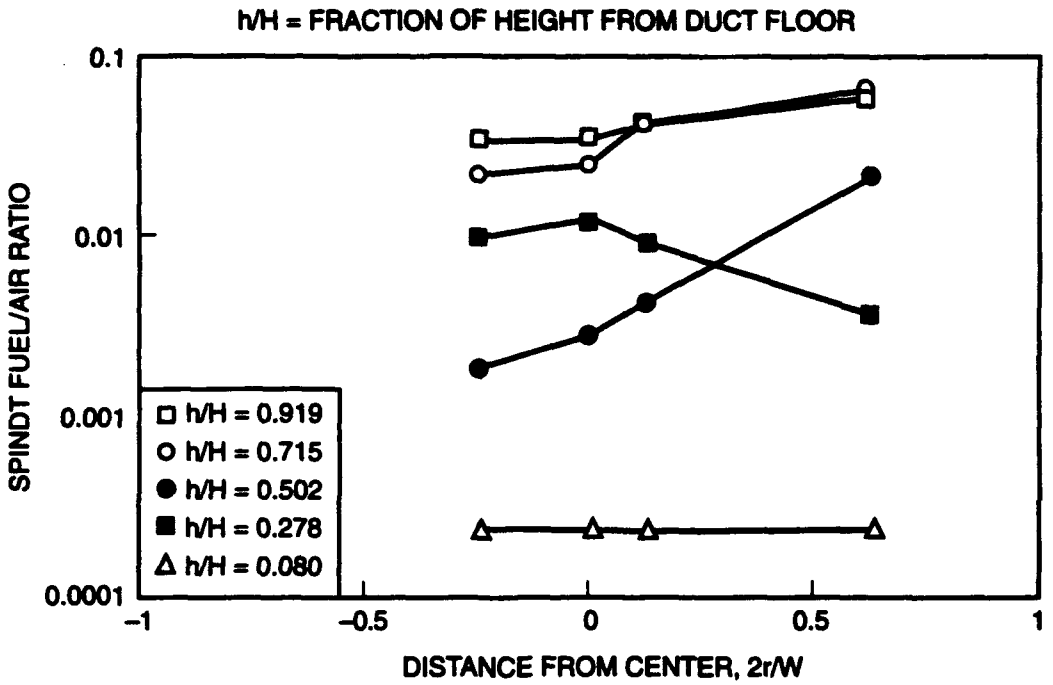

EP310-3-14

Figure 23. Fuel/Air Ratio: Baseline 4 — $W_p/W_s = 0.70$

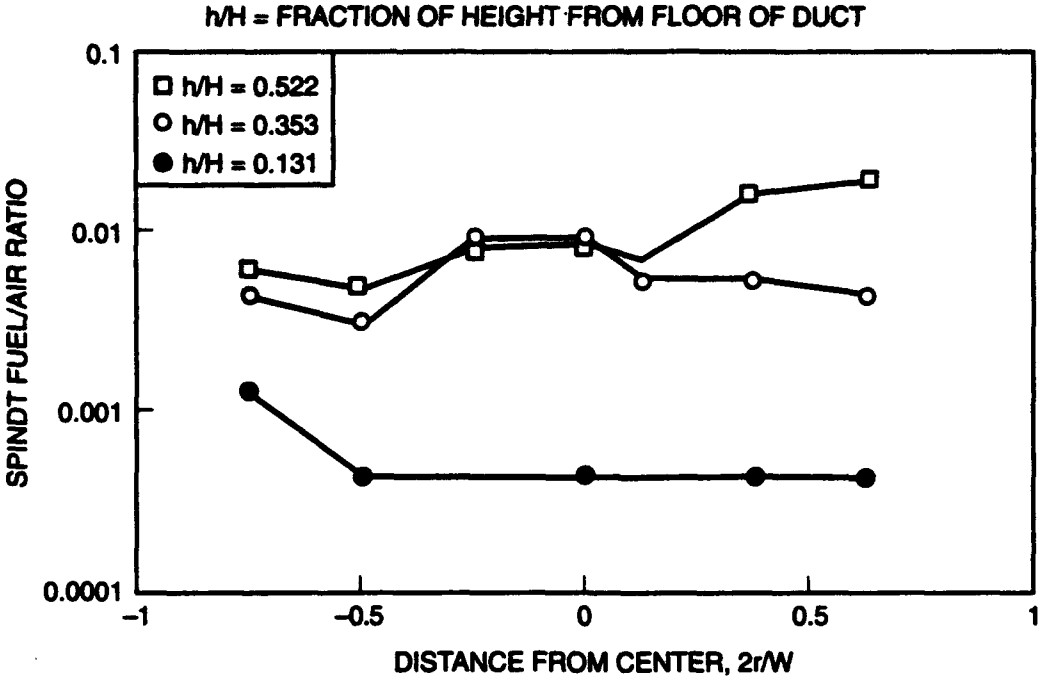

EP310-3-15

Figure 24a. Fuel/Air Ratio: Baseline 4/Alt. 1 — W_p/W_s = 0.30

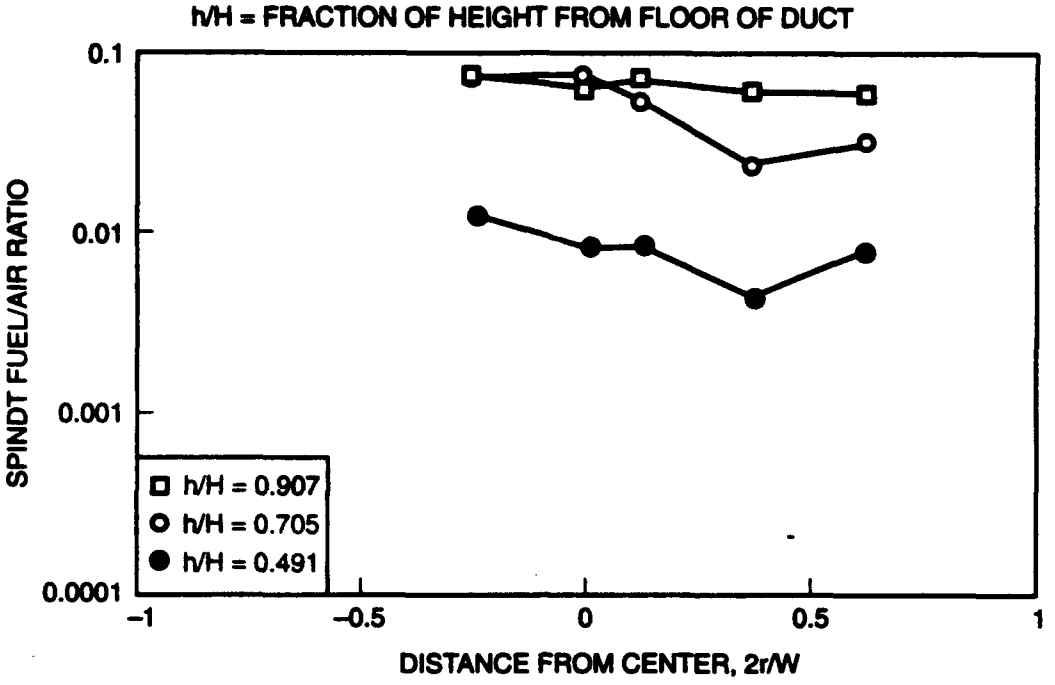

EP310-3-16

Figure 24b. Fuel/Air Ratio: Baseline 4/Alt. 1 — $W_p/W_s = 0.30$

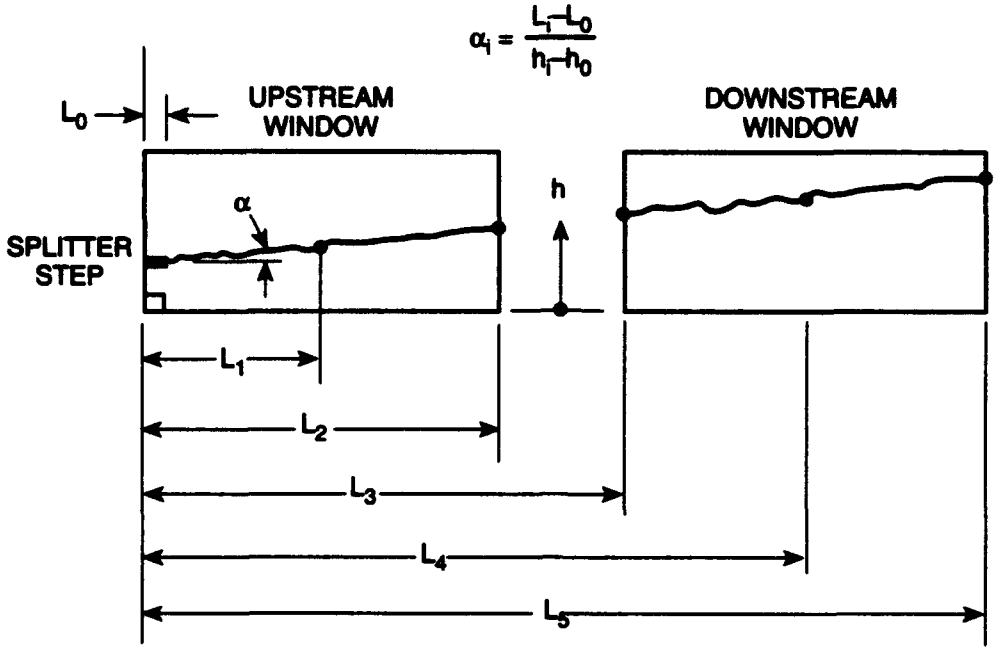

EP310-3-17

Figure 25. Definition of Flame Front Inclination

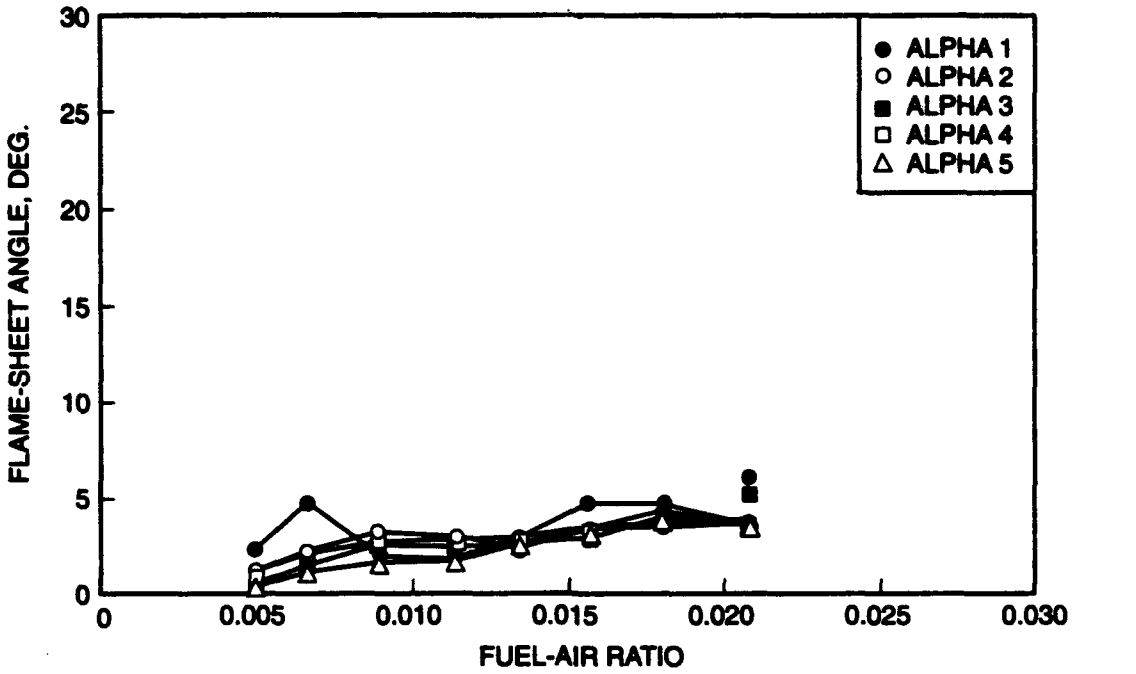

Figure 26a. Flame Angles Developed with Linear Splitter, $W_{pri}/W_{sec} = 0.20$

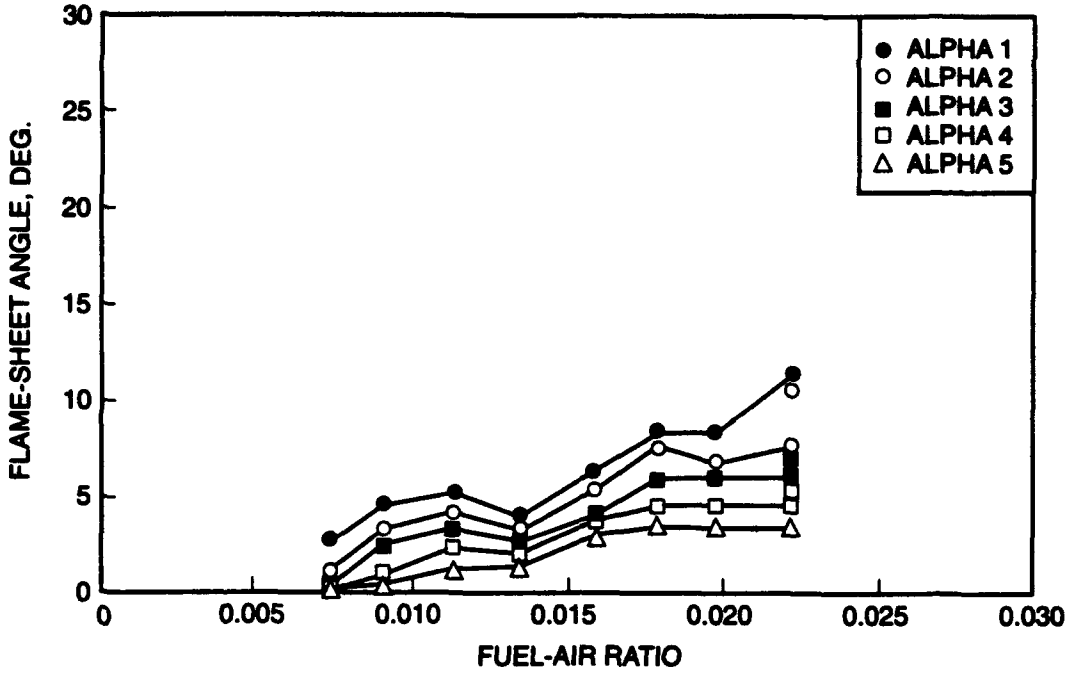

Figure 26b. Flame Angles Developed with Linear Splitter, $W_{pri}/W_{sec} = 0.70$

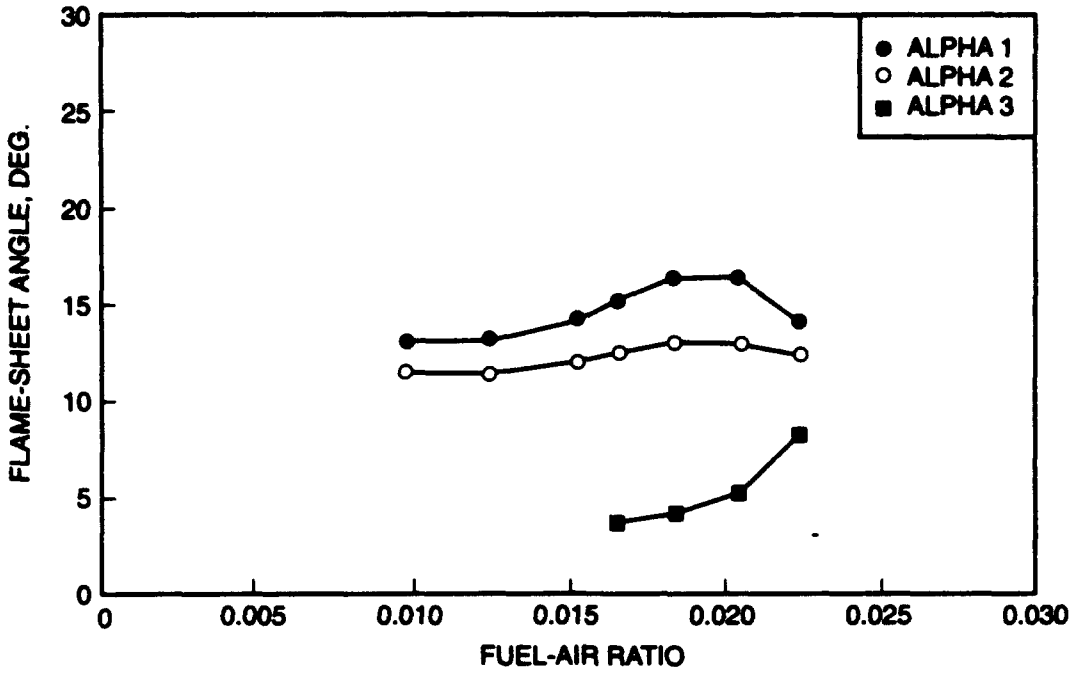

Figure 27a. Flame Angles Developed Using Convoluted Splitter, B4, W_{prf}/W_{sec} = 0.26

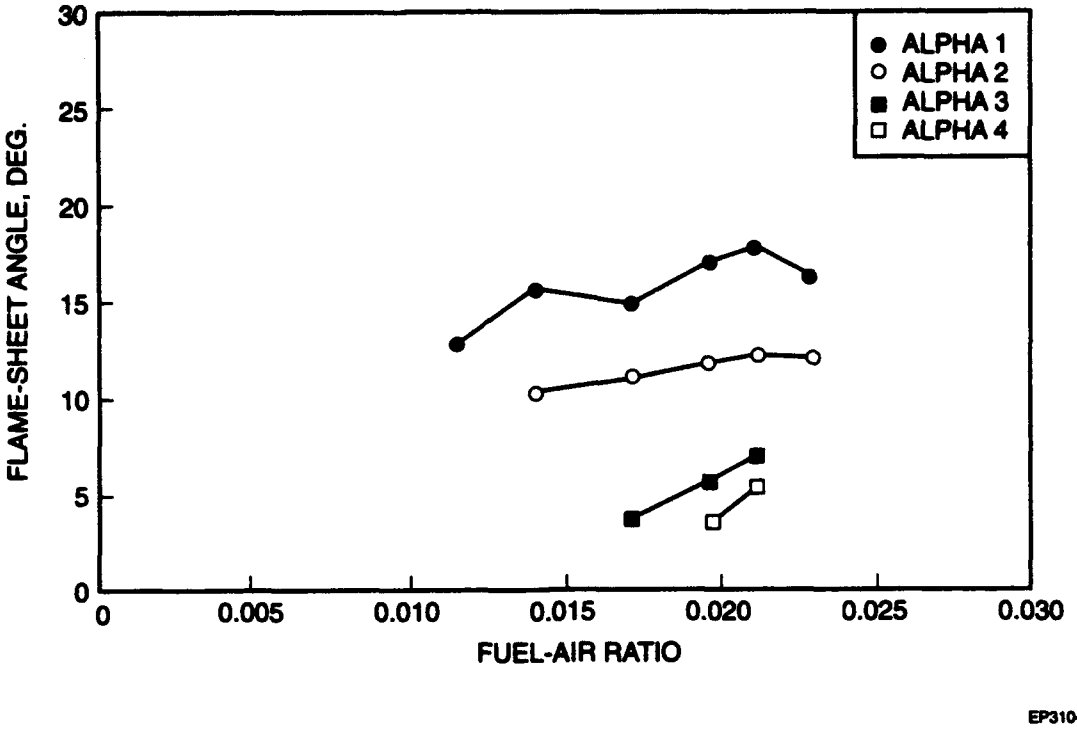

Figure 27b. Flame Angles Developed Using Convoluted Splitter, B4, W_{pri}/W_{sec} = 0.72

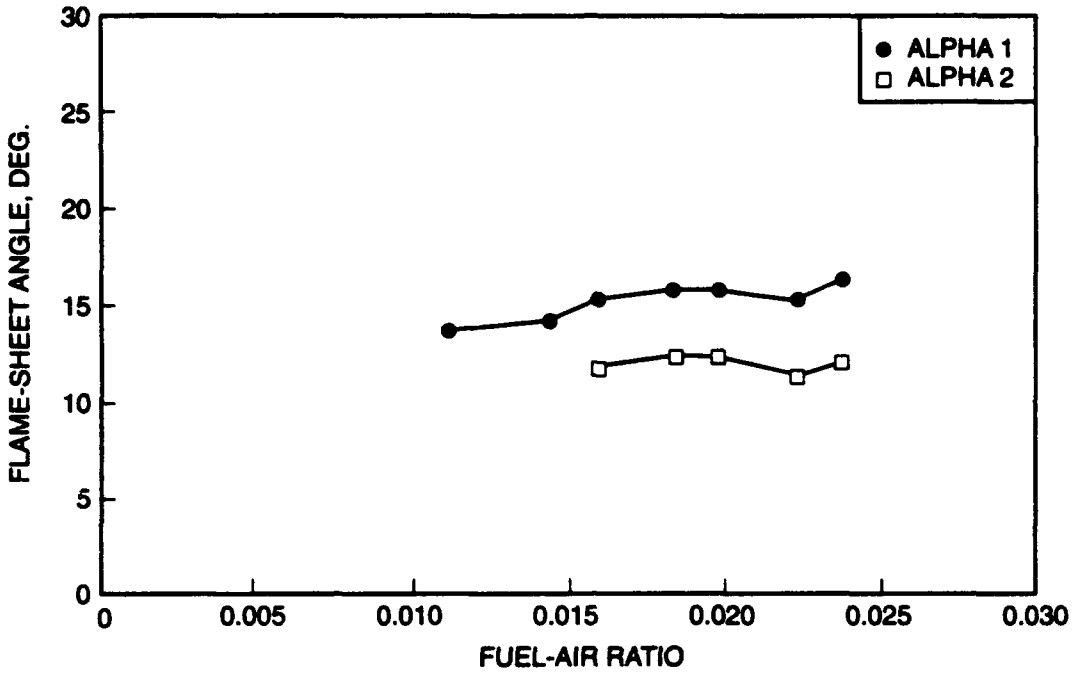

Figure 28a. Flame Angles Developed Using Convoluted Splitter, B4A1, W_{prl}/W_{sec} = 0.27

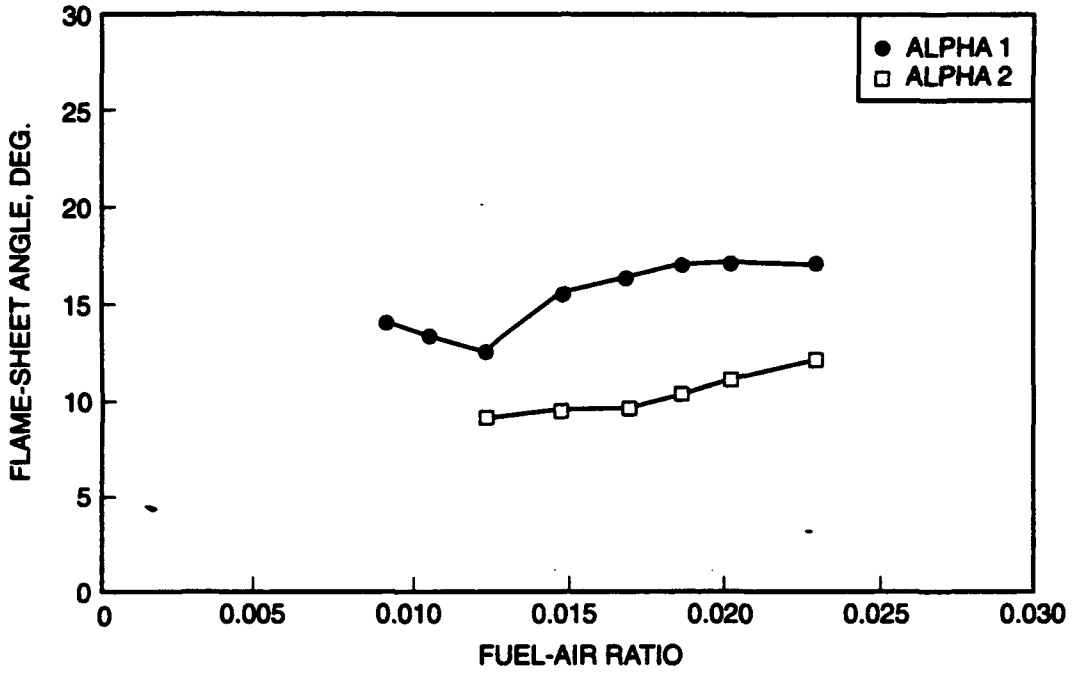

Figure 28b. Flame Angles Developed Using Convoluted Splitter, B4A1, W_{pri}/W_{sec} = 0.76

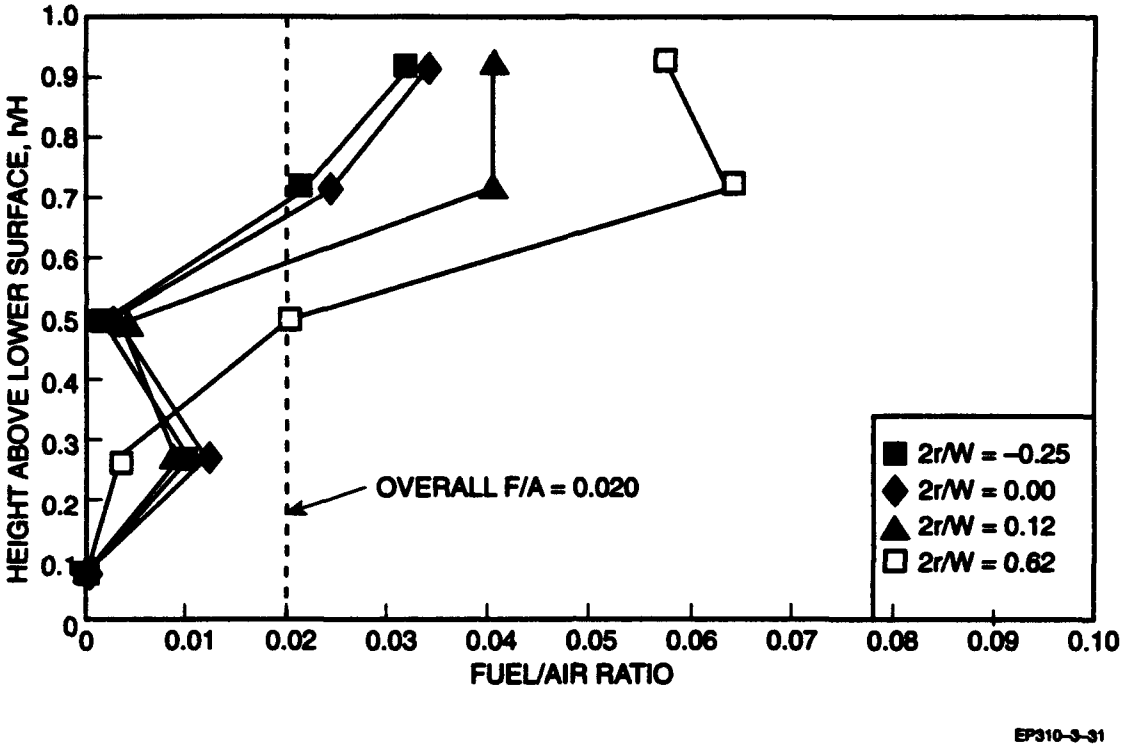

Figure 29. Vertical Fuel-Air Ratio Distribution for Convoluted Splitter, B4 at 27.3 cm from Step. W_{prl}/W_{sec} = 0.7

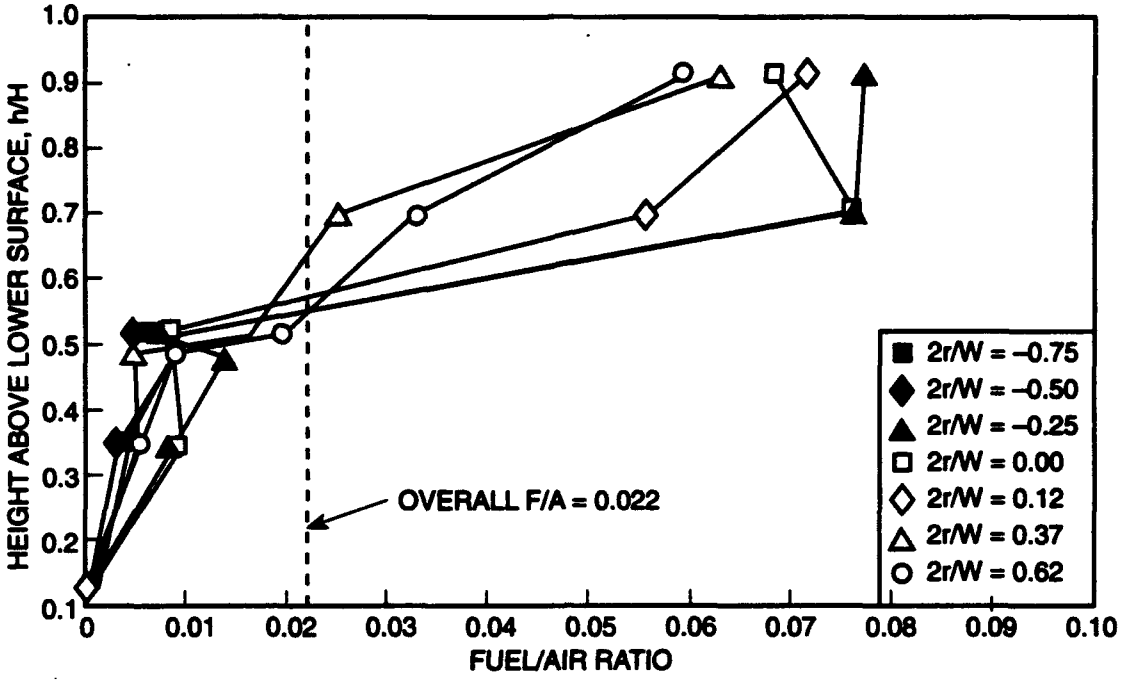

Figure 30. Vertical Fuel-Air Ratio Distribution for Convoluted Splitter, B4A1 at 27.3 cm from Step. W_{prl}/W_{sec} = 0.3

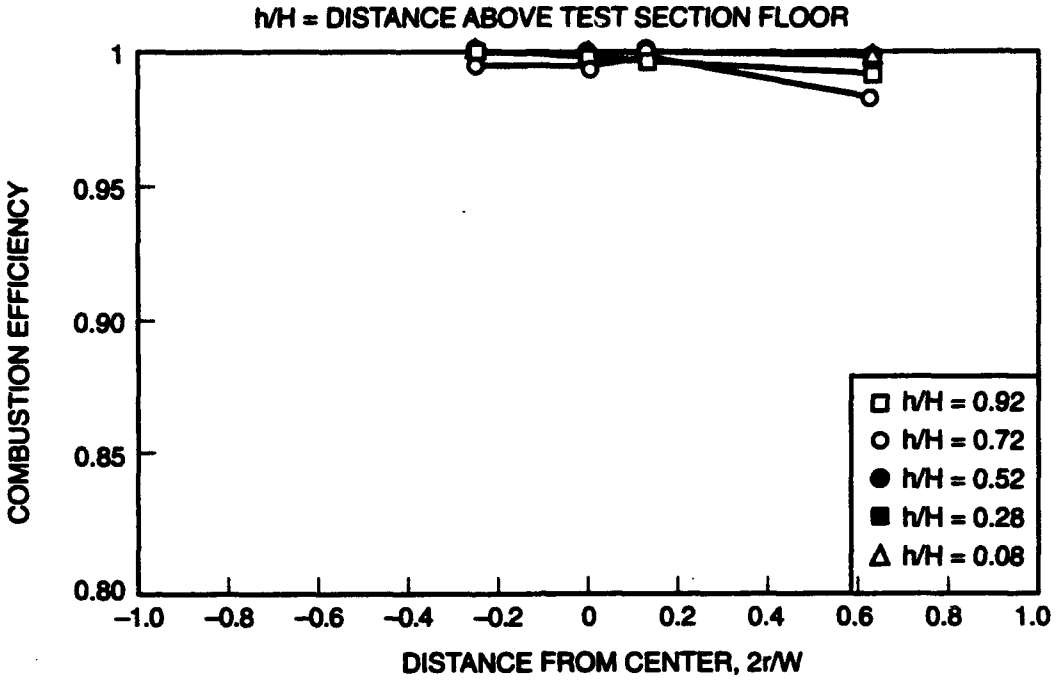

EP310-3-39

Figure 31. Combustion Efficiency: Baseline 4 — $W_p/W_s = 0.70$

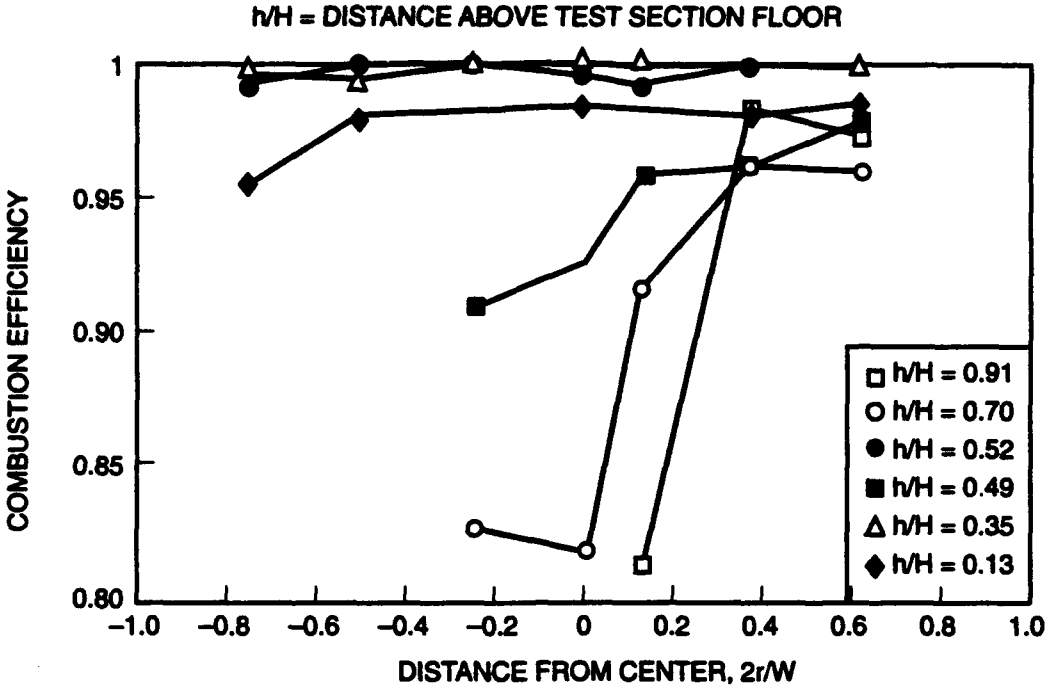

EP310-3-40

Figure 32. Combustion Efficiency: Baseline 4A1 — $W_p/W_s = 0.30$

APPENDIX A - TEST FACILITY
STREAMWISE VORTICITY-STIRRED COMBUSTION

Delivery Systems

Air, nitrogen, and fuel are delivered to the test apparatus which is located in an explosion-proof test cell. Two air sources are available for use in this cell; a nominal 27 atm system that can deliver 9.0 kg/sec of air on a continuous basis and greater flow rates on an intermittent basis. It is possible to heat this air using an indirectly fired heater to a temperature of approximately 530 deg K. A second air source can supply unheated air at a nominal pressure of 41 atm and at flow rates to 2.3 kg/sec.

A 720 kW electric resistance air heater is used to heat the air flow delivered to the flow-preparation section through a pair of high-temperature metering valves. The valves enable the establishment of separately controlled primary and secondary airflows. An orifice plate and a stainless-steel honeycomb flow straightener are placed in both the primary and secondary flows upstream from the test section.

Standard fuel delivery systems which are available include Jet-A, JP-7, propane and several gaseous fuels such as hydrogen and methane. Jet-A is delivered at pressures up to 100 atm. Flow rates are established by dome-loaded pressure regulators; flow rates are monitored using turbine meters.

During this effort, the Jet-A fuel was delivered through a six-orifice airblast atomizer (Fig. A-1) that was designed and fabricated specifically for the current experiment. The fuel injector is situated in the primary flow at a distance of approximately 18 cm. upstream from the rearward-facing step, with the fuel injection directed downstream. The injector air flow rate was maintained at a level corresponding to a pressure differential of approximately 5.5 atm.

Test Apparatus

A general description of the test apparatus was provided in the main body of this report. The apparatus, comprising the air delivery piping, the preparation section, the water-cooled test section and the exhaust ducting comprise a general-purpose combustion research apparatus furnished to the effort by the United Technologies Corporation. Additional features of the apparatus, not addressed previously, are discussed hereunder.

The elevated-temperature air from the two metering valves was delivered to the flow-preparation section, which incorporated a perforated plate and a flow straightener in both the primary and secondary flow passages. As stated above, the fuel injector is located in the lower primary flow passage.

The test section consists of an outer and inner wall, forming a passage through which cooling water is passed. This cooling water also passes between two plates of quartz glass that, together, form the top and sidewalls of the test section and provide optical access to the interior of the test section. The inner glass plate is approximately 19-mm thick and the outer plate is approximately 25-mm thick. The separation between the inner and outer plates is approximately 3 mm. The lower wall of the test section is also water-cooled and contains provision for the installation of the spark-initiated, hydrogen/air torch used to ignite the fuel-air mixture.

The design of the window installation represents a departure from conventional window installations with regard to the internal pressure that is imposed (7 atm.) and, in particular, with respect to the size of the windows (approximately 12.7 cm x 30.5 cm). The windows provide optical access to a combustion region in which local temperatures corresponding to stoichiometric combustion of the fuel and air are developed. Heat transfer calculations indicated that air would not provide adequate cooling of the windows. Similar calculations indicated the desirability of using water although very high temperature gradients across the glass thickness would be developed.

The combustion products are passed from the test section to an exhaust duct through a special water-cooled transition section in which a window is installed that provides a view of the combustion region from a downstream location. This window is removed when the emissions-sampling rake is installed to provide a point of support for the rake assembly.

Control System

The control system comprised a combination of manual and micro-computer-based controls. Owing to the differences in procedures required for acquiring visual records of the flame shapes and for obtaining emissions samples, most of the test procedure was affected manually. The function of the computer-based system was to ensure the proper sequencing of the ignition operation and to provide the necessary interlocks to affect shutdown of the equipment in the event of a loss in coolant flow to the test apparatus. It was especially important to monitor the coolant flow to the quartz windows and to terminate the test in the event that a window failure occurred.

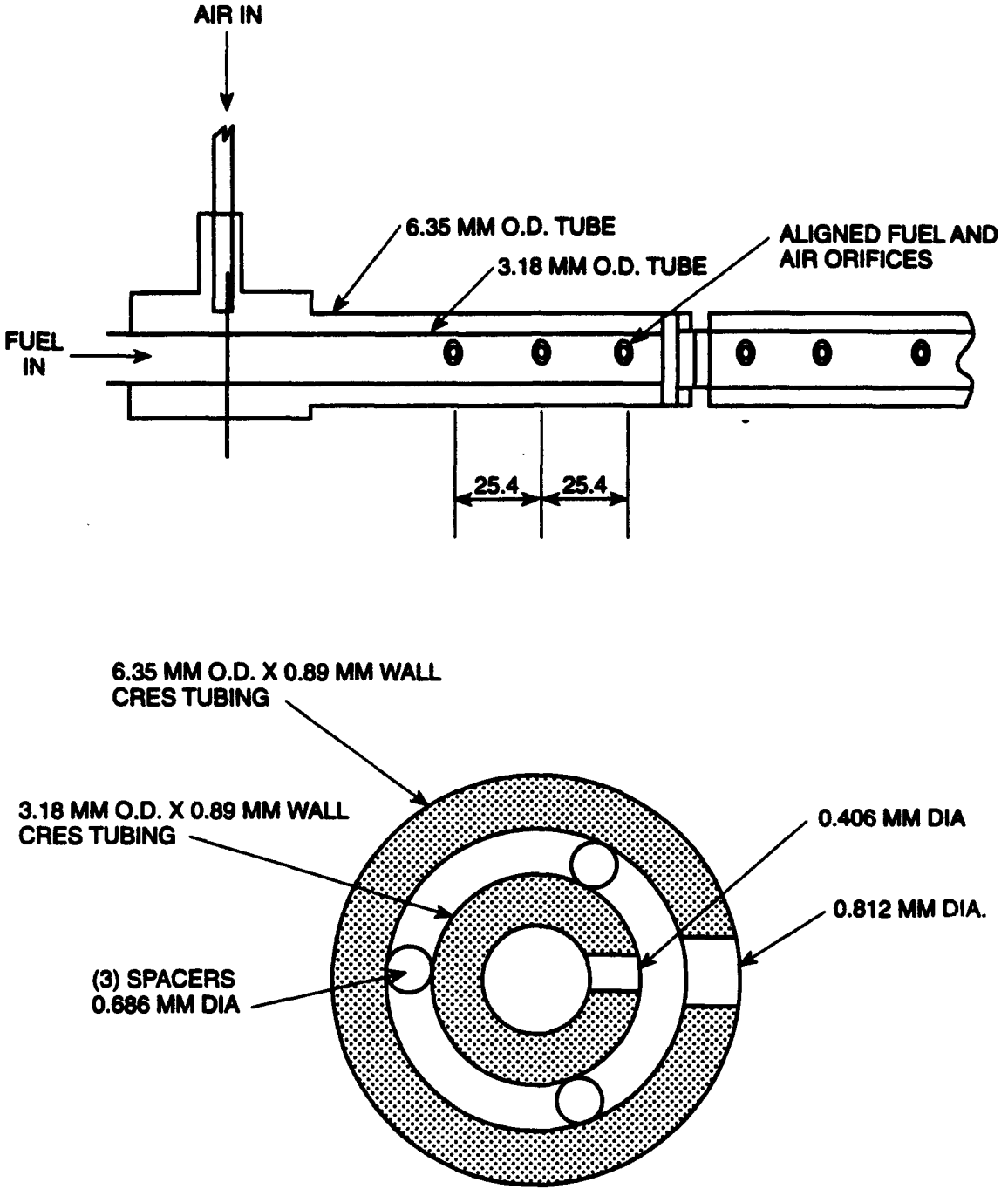

Figure A-1. SVS Fuel Injector

APPENDIX B - EMISSIONS SAMPLING INSTRUMENTATION

The emissions sampling rake, incorporating the seven aerodynamically quenching probes, was provided by United Technologies Corporation. The rake assembly comprised two separate subassemblies, a probe support and the rake with its water-cooled "sting". The probe support was inserted through a ball and socket that was part of a flange which replaced the aft window assembly during sampling tests, as shown in Fig. B-1. The water-cooled sting, shown in Fig. B-2, was supported within the probe support and sealed with o-rings. This arrangement allowed sliding of the sting within the support to enable axial relocation of the rake from test to test. A water-cooled yoke encircled the support(Fig. B-1) and was held in place with vertically oriented, water-cooled push rods. Vertical traverse of the rake was provided using a Velmex Series MB2500 Unislide traversing mechanism. A Velmex Model 86MM controller was programmed to drive the traversing mechanism.

The seven quenching probes included in the rake in Fig. B-3 were cooled using the water that passed from the rake sting into the wedge that formed the rake and from there back into the rake sting. None of the cooling water was exited into the gas flow path.

The samples from the probes were delivered individually, using a series of valves, to the UTRC Emissions System, depicted schematically in Fig. B-4. All transfer lines between the rake and the emissions analyzers were maintained at a temperature of approximately 420 K.

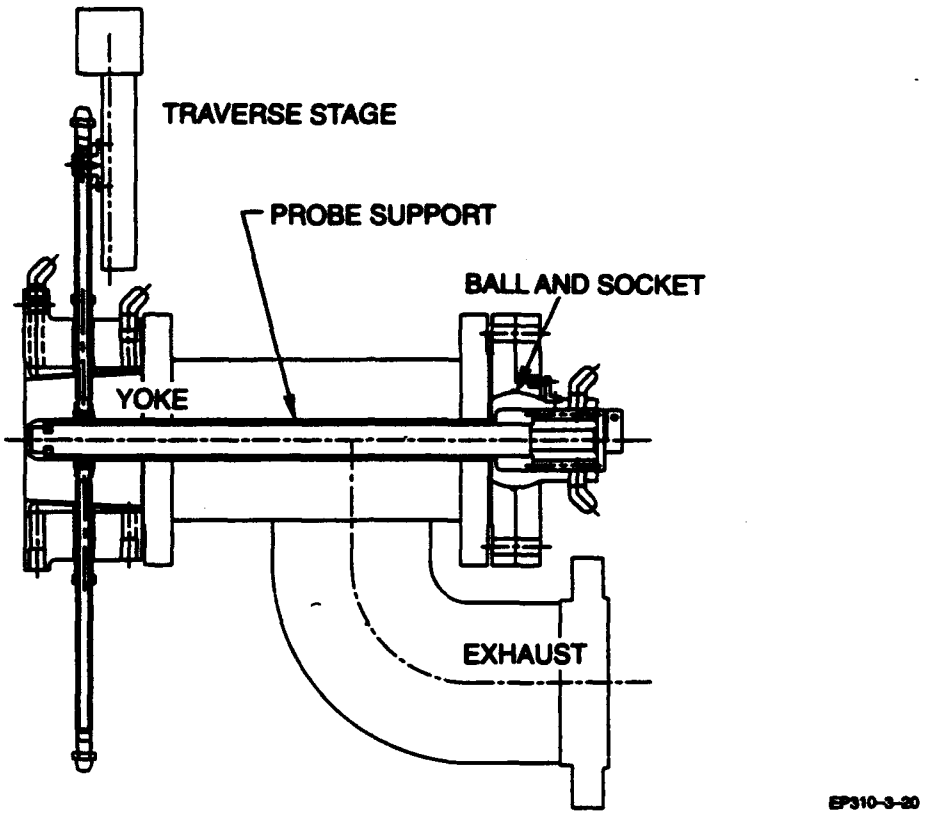

Figure B-1. Emission Probe Installation

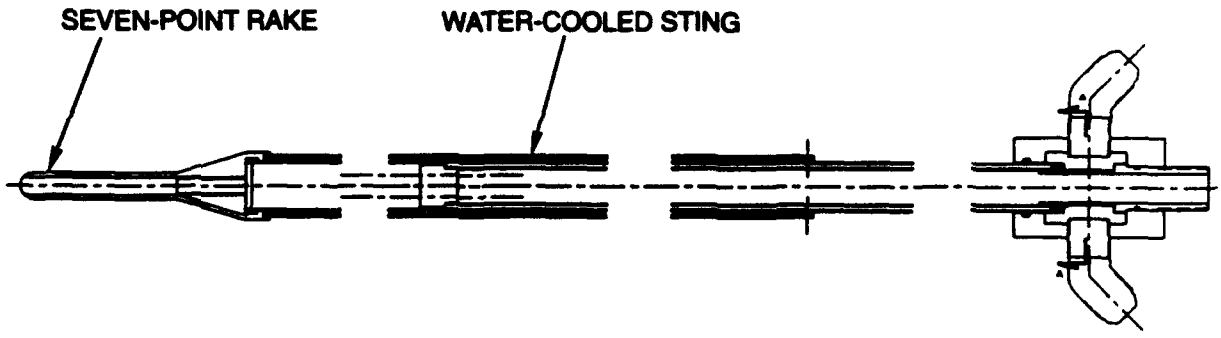

EP310-3-21

Figure B-2. Emission Sampling Probe

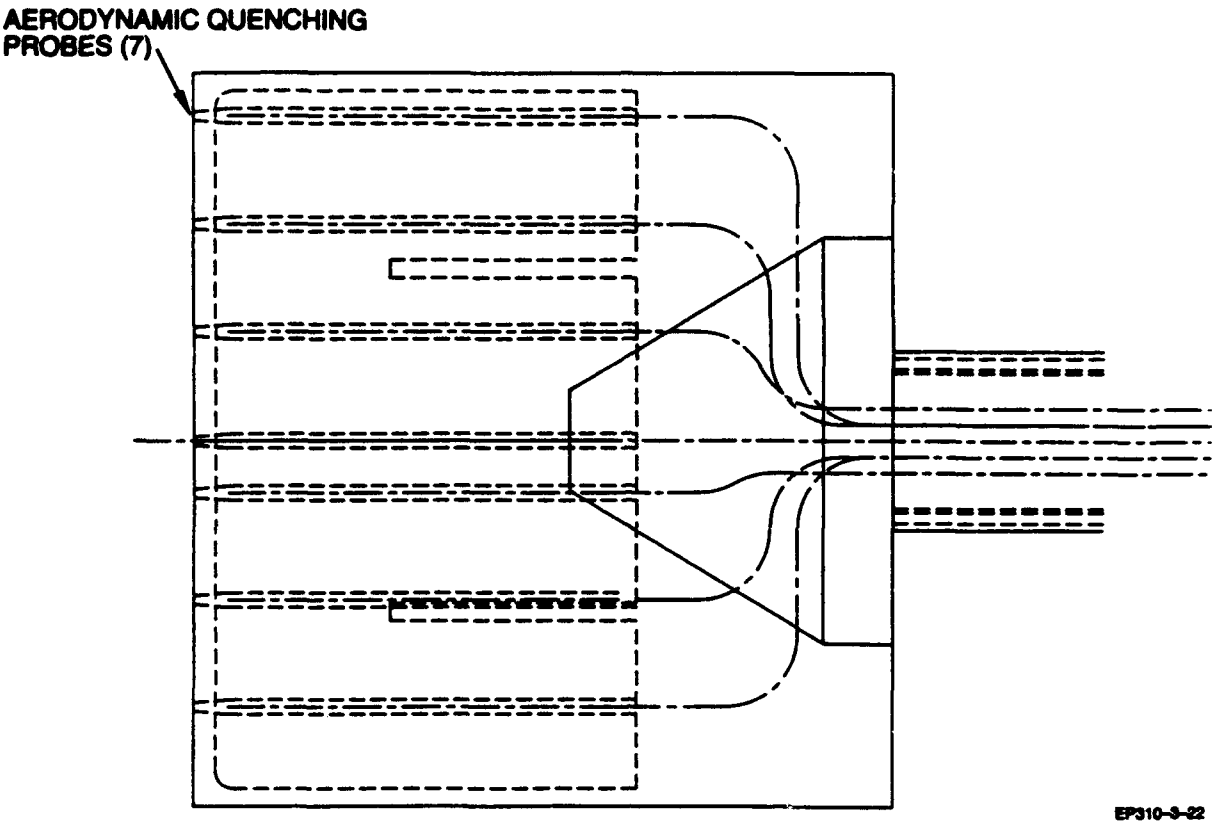

Figure B-3. Emission Sampling Rake

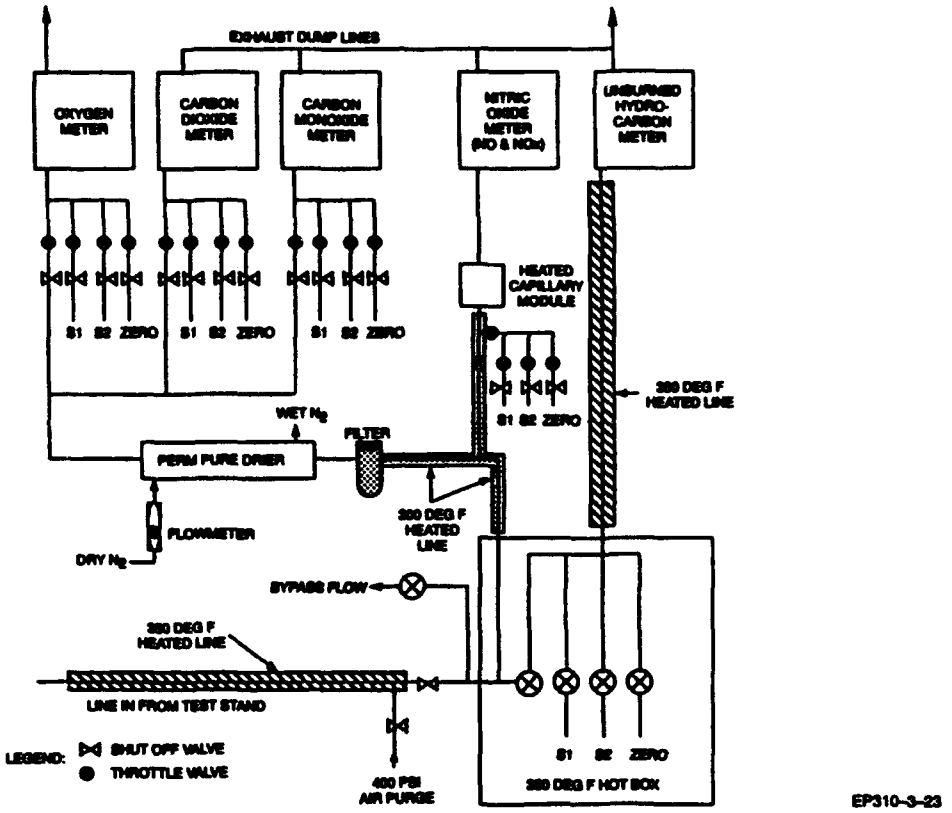

Figure B-4. UTRC Emissions System

APPENDIX C - FLAME ENVELOPES

Reproductions of images of flame shapes, derived from the video-taped records are presented in Figs. C-1 through C-6. The variation of the shape of the flame produced during combustion of Jet-A at several fuel-air ratios, using the linear splitter with the 2.5-cm. high step is shown in Fig. C-1. The level of W_{prf}/W_{sec} = 0.8. The hatched regions in the diagrams correspond to regions in the videotaped images in which the flame appeared as bright yellow. The densely shaded areas correspond to the areas in which the flame appeared as a less-luminous orange. The unhatched, unshaded area at the top of each frame was essentially transparent.

Figure C-2 portrays the flame shapes produced during combustion of Jet-A fuel at several fuel-air ratios, recorded in tests conducted using the convoluted splitter, B4. The level of W_{prf}/W_{sec} = 0.75. The scheme used in Fig. C-1 to denote the regions of the flame applies to this figure. Note the more extensive "coverage" of the flow area by the flame regions, compared with the coverage provided by the linear-splitter flame.

Figures C-3 through C-6 compare the flame shapes recorded for the convoluted splitters, B4 and B4A1. In Figs. C-3 and C-4, the flame shapes developed during combustion at a fuel-air ratio of approximately 0.02 are compared. In the first of these two figures, the level of W_{prf}/W_{sec} = 0.75. In the second figure, Fig. C-4, a similar comparison is made at a level of W_{prf}/W_{sec} = 0.27. In Figs. C-5 and C-6, the flame shapes are compared for an overall fuel-air ratio of approximately 0.01 when the levels of W_{prf}/W_{sec} = 0.73 and 0.27, respectively.

In this figure, as well as in those described below, the leftmost edge of the upstream window is 19 mm upstream from the rearward-facing step. Each window is approximately 30.5-cm. wide and 12.7-cm. tall. The upstream and downstream edges of the downstream window are at distances of approximately 44.5 and 75 cm. from the step.

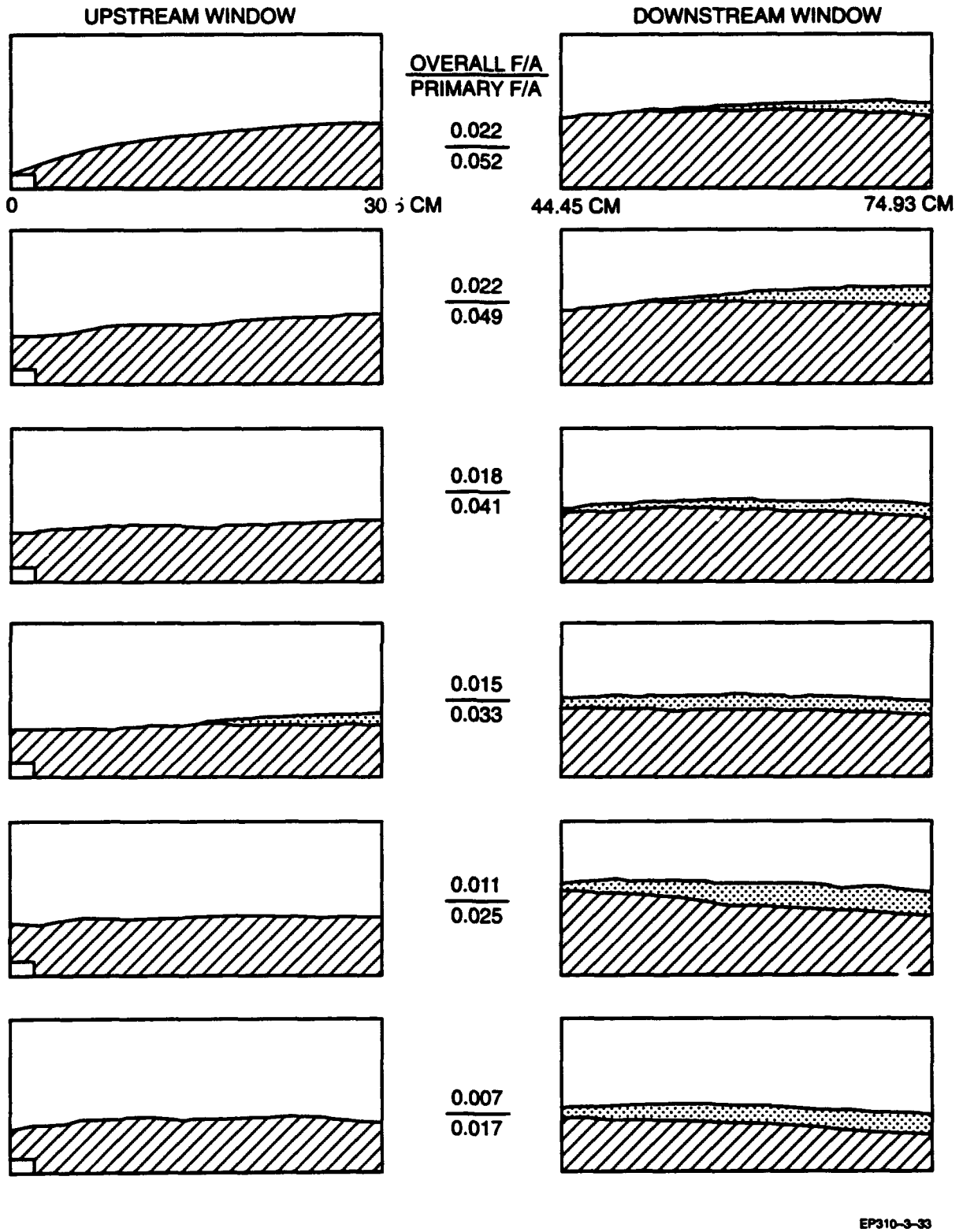

Figure C-1. Flame Shapes Produced by Linear Splitter Plate at Indicated Fuel-Air Ratios. $W_{pri}/W_{sec} = 0.8$

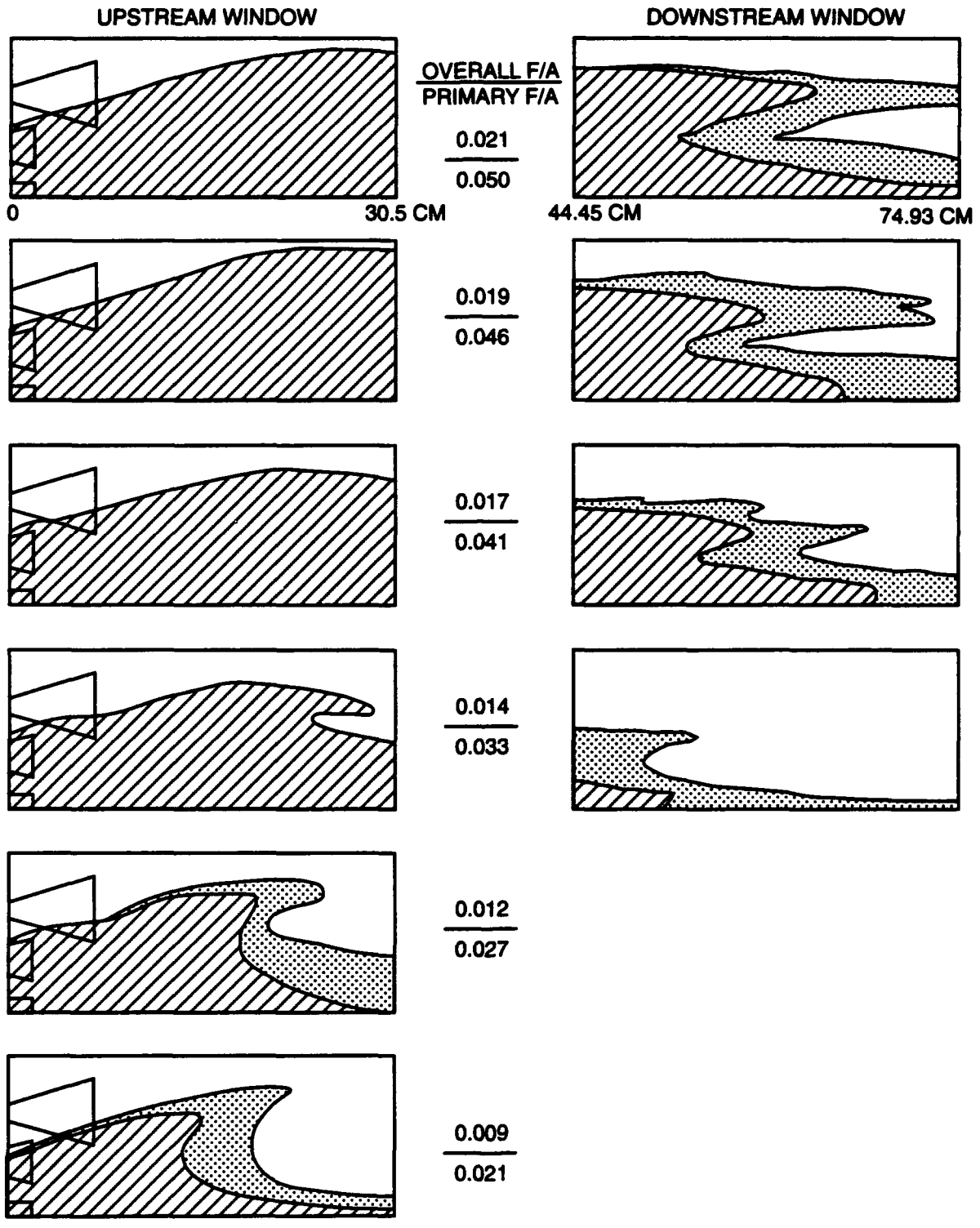

Figure C-2. Flame Shapes Produced by Convoluted Splitter Baseline 4 at Indicated Fuel-Air Ratios. W_{prl}/W_{sec} = 0.73

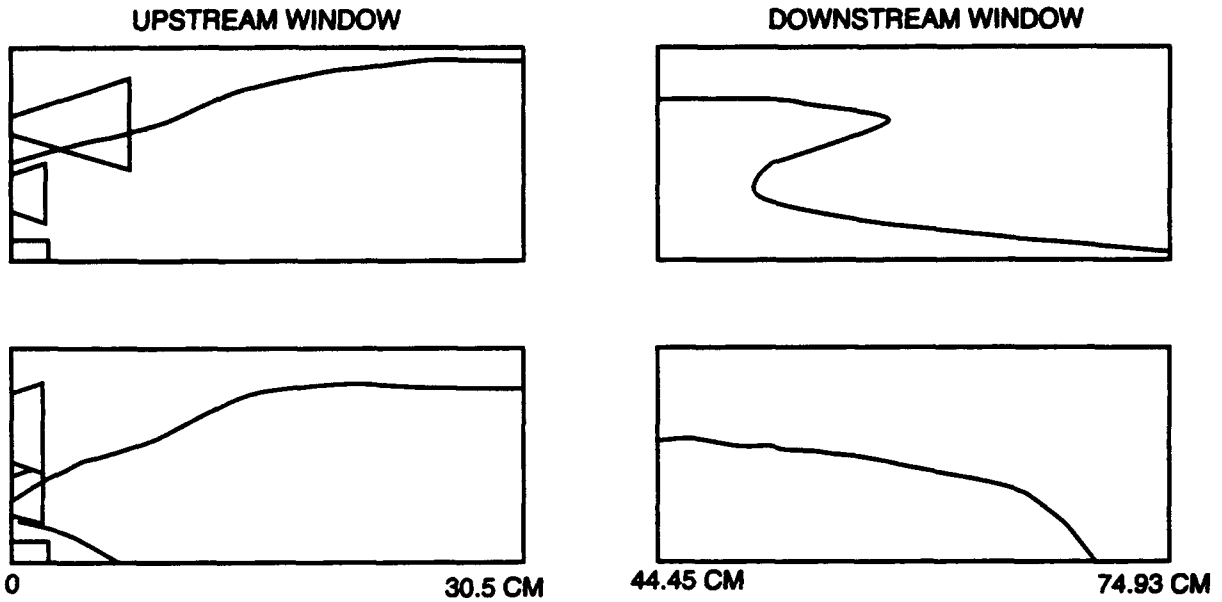

Figure C-3. Comparison of Flame Shapes Produced by Convoluted Splitters B4 (Top) and B4A1 (Bottom) — Overall F/A = 0.02, W_{pri}/W_{sec} = 0.75

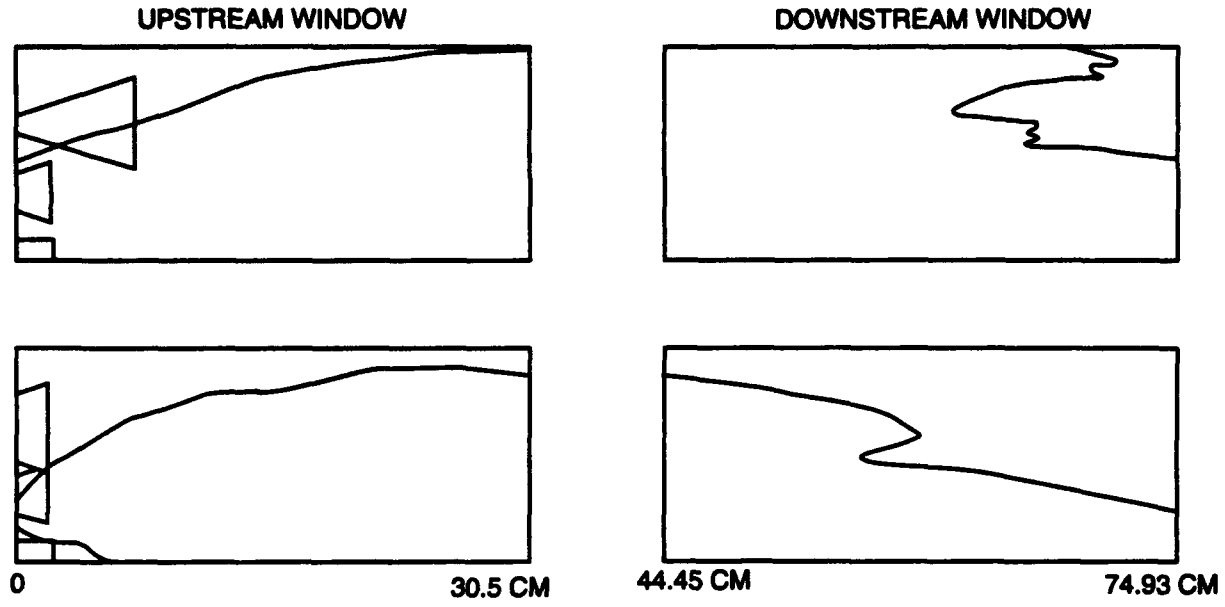

Figure C-4. Comparison of Flame Shapes Produced by Convoluted Splitters B4 (Top) and B4A1 (Bottom) — Overall F/A = 0.02, W_{prl}/W_{sec} = 0.27

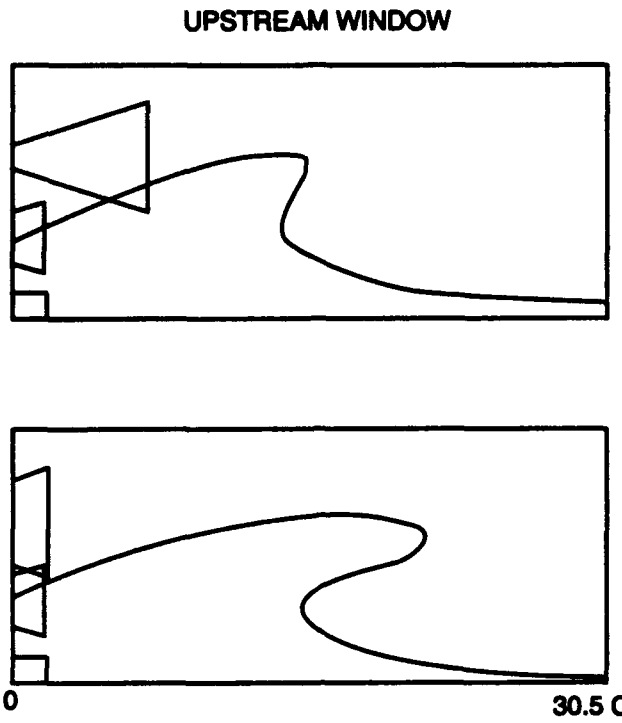

Figure C-5. Comparison of Flame Shapes Produced by Convoluted Splitters B4 (Top) and B4A1 (Bottom) — Overall F/A = 0.01, W_{prl}/W_{sec} = 0.73

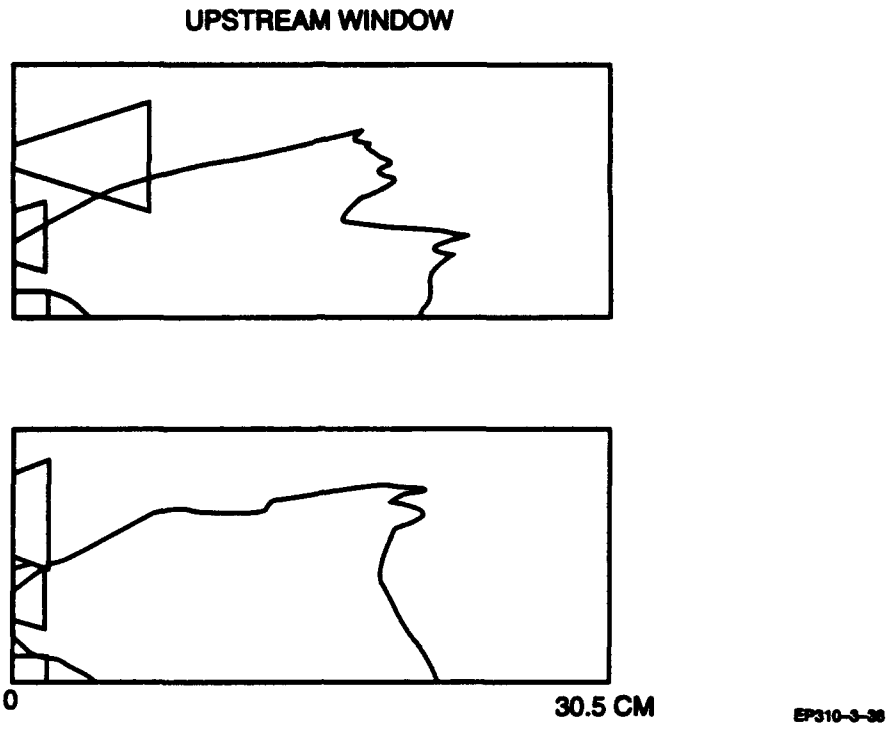

Figure C-6. Comparison of Flame Shapes Produced by Convoluted Splitters B4 (Top) and B4A1 (Bottom) — Overall F/A = 0.01, W_{prl}/W_{sec} = 0.27

REPORT DOCUMENTATION PAGE

Form Approved
OMB No. 0704-0188

1. AGENCY USE ONLY (Leave blank)	2. REPORT DATE	3. REPORT TYPE AND DATES COVERED
	November 1993	

4. TITLE AND SUBTITLE
Study of Streamwise-Vorticity-Stirred Combustion

5. FUNDING NUMBERS

6. AUTHOR(S)
Peschke, William T.
McVey, John B.

7. PERFORMING ORGANIZATION NAME(S) AND ADDRESS(ES)
United Technologies Research Center
400 Main Street
East Hartford, CT 06108

8. PERFORMING ORGANIZATION REPORT NUMBER
ARL-CR-141

9. SPONSORING/MONITORING AGENCY NAME(S) AND ADDRESS(ES)
U. S. Army Research Office
P. O. Box 12211
Research Triangle Park, NC 27709-2211

10. SPONSORING/MONITORING AGENCY REPORT NUMBER
NASA CR 194450

11. SUPPLEMENTARY NOTES
The view, opinions and/or findings contained in this report are those of the author(s) and should not be construed as an official Department of the Army position, policy, or decision, unless so designated by other documentation.

12a. DISTRIBUTION/AVAILABILITY STATEMENT
Approved for public release; distribution unlimited.

12b. DISTRIBUTION CODE

13. ABSTRACT (Maximum 200 words)

Experiments were conducted to establish the effects of the introduction of streamwise vorticity in combusting flows modelling those developed within small gas turbine engines. The objective of the effort was to determine whether this combustion concept has the potential for improving the volumetric heat release rates. Water flow-visualization tests were performed to evolve lobed mixer configurations that, while generating vortex arrays within both the primary and secondary streams, would also provide rapid intermixing between the streams. Combustion experiments were carried out in a high-pressure (7 atm) combustion apparatus. Direct observation and gas sampling were employed to characterize the fuel-air ratio distribution effected by the mixers. Flame geometries were compared with those developed during shear-layer combustion occurring downstream from a conventional splitter plate. As contrasted with the 5- to 7-degree flame front angles that occurred during shear layer combustion, the flame front angles developed during combustion using the lobed mixers were more than twice as great, attaining levels approaching 20 degrees.

14. SUBJECT TERMS	15. NUMBER OF PAGES
Flame Propagation, Combustion, Turbulent Combustion, Vorticity, Streamwise Vorticity	71
	16. PRICE CODE

17. SECURITY CLASSIFICATION OF REPORT	18. SECURITY CLASSIFICATION OF THIS PAGE	19. SECURITY CLASSIFICATION OF ABSTRACT	20. LIMITATION OF ABSTRACT
UNCLASSIFIED	UNCLASSIFIED	UNCLASSIFIED	UL